



# The protohistoric briquetage at Puntone (Tuscany, Italy): A multidisciplinary attempt to unravel its age and role in the salt supply of Early States in Tyrrhenian Central Italy

Jan Sevink<sup>a,\*</sup>, Gerard Muijzer<sup>a</sup>, Ilenia Arienzo<sup>b</sup>, Angela Mormone<sup>b</sup>, Monica Piochi<sup>b</sup>, Luca Alessandri<sup>c</sup>, Rutger L. van Hall<sup>a</sup>, Sanne W.L. Palstra<sup>d</sup>, Michael W. Dee<sup>d</sup>

<sup>a</sup> Institute for Biodiversity and Ecosystem Dynamics (IBED), University of Amsterdam, Science Park 904, 1098 XH Amsterdam, Netherlands

<sup>b</sup> Istituto Nazionale di Geofisica e Vulcanologia (INGV), Via Diocleziano 328, 80124 Napoli, Italy

<sup>c</sup> Groningen Institute of Archaeology (GIA), University of Groningen, Poststraat 6, 9712 ER Groningen, Netherlands

<sup>d</sup> Centre for Isotope Research (CIO), ESRIG, University of Groningen, Nijenborgh 6, 9747 AG Groningen, Netherlands

## ARTICLE INFO

### Keywords:

Briquetage  
Central Italy  
Early states  
Radiocarbon dating  
Carbonates  
Organic matter

## ABSTRACT

While processes involved in the protohistoric briquetage at Puntone (Tuscany, Italy) have been reconstructed in detail, the age of this industry remained uncertain since materials suited for traditional dating ( $^{14}\text{C}$  dating on charcoal and typological dating of ceramics) were very scarce. We attempted to assess its age by radiocarbon dating organic matter and carbonates in strata that were directly linked to the industry. Microbial DNA and C isotope analyses showed that the organic matter is dominantly composed of labile organic matter, of which the age is coeval with the briquetage industry. Carbonates had a complex origin and were overall unsuited for radiocarbon dating: Shells in process residues exhibited a large, uncertain 'marine reservoir effect', hampering their use for dating the industry; the secondary carbonates in these residues had a quite varied composition, including much more recent carbonate that precipitated from infiltrated lateral run-off, as could be concluded from C and Sr isotope analyses. Dates found that were deemed reliable (c. 1000–100 cal BCE) show that this ancient industry, which started in the Late Bronze Age - Early Iron Age (1107–841 cal BCE), extended into the Roman Republican period and was contemporary with the saltern-based larger scale salt industry in Central Lazio.

## 1. Introduction

In ancient times, in Central Italy a flourishing salt industry existed, as testified by the presence of protohistoric production sites in all larger Tyrrhenian coastal plains. These included the Piombino/Follonica area (Fig. 1), where excavations revealed major salt production complexes (Barbaranelli, 1956; Aranguren, 2002; Baratti, 2010; Aranguren & Castelli, 2011; Giroladini, 2012; Aranguren et al., 2014). This industry flourished against the background of the birth of the Early States during the Iron Age (c. 1000 BCE, Bintliff, 2016), when this region witnessed strong demographic growth and an associated increase in the salt demand.

Harding (2014), reviewing ancient salt production, described the

Tyrrhenian coast of Italy as a 'solar evaporation zone' where salt was produced by evaporation of seawater in shallow artificial salt pans. This technique requires a climate with prolonged dry and warm periods and is described as the saltern technique. The statement by Harding is evidently true for Roman times (Lowe, 2018), as we also know from the ancient sources (Plin. NH XXXI, 73; Rut. Namat. 1.475–478). However, at Puntone Campo da Gioco (see Fig. 1) a protohistoric site was discovered (Aranguren et al. 2014) where salt was produced by briquetage (see e.g. Hocquet & Sarrazin, 2006; Harding, 2013; Tencariu et al., 2015). This technique involves boiling brine in ceramic vessels over a fire to produce massive salt. At the end of the process, the vessels needed to be broken to extract the salt-cake. Thus massive amounts of ceramic debris belonging almost exclusively to jars are usually present

\* Corresponding author.

E-mail addresses: [j.sevink@uva.nl](mailto:j.sevink@uva.nl) (J. Sevink), [g.muijzer@uva.nl](mailto:g.muijzer@uva.nl) (G. Muijzer), [ilenia.arienzo@ingv.it](mailto:ilenia.arienzo@ingv.it) (I. Arienzo), [angela.mormone@ingv.it](mailto:angela.mormone@ingv.it) (A. Mormone), [monica.piochi@ingv.it](mailto:monica.piochi@ingv.it) (M. Piochi), [Lalessandri@rug.nl](mailto:Lalessandri@rug.nl) (L. Alessandri), [R.L.vanHall@uva.nl](mailto:R.L.vanHall@uva.nl) (R.L. van Hall), [s.w.l.palstra@rug.nl](mailto:s.w.l.palstra@rug.nl) (S.W.L. Palstra), [m.w.dee@rug.nl](mailto:m.w.dee@rug.nl) (M.W. Dee).

<https://doi.org/10.1016/j.jasrep.2021.103055>

Received 26 February 2021; Received in revised form 10 May 2021; Accepted 20 May 2021

Available online 7 June 2021

2352-409X/© 2021 The Author(s). Published by Elsevier Ltd. This is an open access article under the CC BY license (<http://creativecommons.org/licenses/by/4.0/>).

in these specialised areas. All over Europe sites with this characteristic have been found, of which the earliest date from the VI millennium BCE, whilst the largest diffusion of the briquetage technique occurs between the Iron Age and the Roman times (Harding, 2013). In Italy, a significant concentration of briquetage sites has been reported along the Tyrrhenian coast, in a time-span ranging from the Middle Bronze Age to the Iron Age (17th to 8th century BCE; Alessandri et al., 2019).

Fig. 2 shows the Puntone site as identified in a geophysical survey and details of relevant features, while Fig. 3 depicts the production processes as reconstructed by Sevink et al. (2021) to which reference is made for their full description. At Puntone, brine was produced by leaching saline sediment, taken from the nearby lagoon, over a sieve that was placed above a pit. Brine collected in this pit was subsequently used for salt production by briquetage. Several pits were used, dug into the impermeable deep clay soil of the alluvial fan slope on which the Puntone site is located, just above the lagoon. Pits gradually became filled with fine sediment passing the sieve, ultimately hampering further operation of the system and requiring ‘cleaning’ to allow for their proper use as brine collector. This sequence of processes – leaching of lagoonal sediment and cleaning of a pit once largely filled with fine sediment – was repeated over time.

The complex history of the site is best recorded in these brine pits and associated stratigraphic units, including the fan-shaped dumps of processed sandy sediment (see Fig. 2). This is well illustrated by the pit studied in detail (see Fig. 4). A large number of stratigraphic units could be identified based on criteria such as their colour, texture and composition. Stratigraphic boundaries were very distinct and allowed for identification of four phases, indicated in Fig. 4a. The pit reached its largest dimensions at the start of phase 2 when the original pit was cleaned, destroying any trace of the earlier pit, but strata linked to that earlier phase (phase 1) were well-preserved. The phase 3 pit was smaller and only the lower strata of its fill were preserved upon its cleaning. Interestingly, at the onset of phase 4 the wall of the cleaned pit was plastered with clay in a presumed attempt to reduce infiltration losses. By the end of the ultimate phase (phase 4) the system was abandoned,

leaving behind a fully filled pit.

An important question is whether this briquetage system represents an early small-scale system of salt production that over time was replaced by salterns or a rather artisanal coeval salt production method. Answers to that question evidently require adequate dates for the currently known briquetage sites in Central Italy. However, at sites studied thus far, both typologically datable ceramics and more traditional materials that can be readily used for radiocarbon dating were generally found to be rare or absent (Attema & Alessandri, 2012), preventing a precise dating. This also holds for the Puntone site.

At Puntone, charcoal in a stratum from the earliest phase 1 (unit 16, see Fig. 4) was radiocarbon dated to 1107–841 cal BCE (Sevink et al., 2021), in line with an earlier radiocarbon dating to 902–786 cal BCE by Aranguren et al. (2014). According to Van der Plicht & Nijboer (2018) this phase would date to the Italian late Final Bronze Age to Early Iron Age, in congruence with the dating based on the typology of the associated ceramics (Aranguren et al., 2014; Cinquegrana, in prep.). Attempts to date later phases by ceramic typology were in vain, as were attempts to radiocarbon date charcoal or macro plant remains in younger archaeological strata; these have not been encountered at the Puntone site thus far. A rural Roman villa was constructed on top of the remains of the briquetage industry, which was dated to the 1st century BCE, setting a *terminus ante quem* (Balestri and Magagnoli, 1981; Paribeni, 1985).

The foregoing implies that an answer to the question whether the briquetage was coeval or not with the saltern-based production, if to be settled by radiocarbon dating, would require the dating of less usual materials, encountered in the pit fills and associated sediments. In the first place, upon evaporation of a brine the first component to precipitate is calcium carbonate (Usiglio, 1849). Such carbonate might allow for radiocarbon dating of production residues. Secondly, other carbonates encountered in these residues are biogenic (i.e. shells), which can also be radiocarbon dated, though such dating is potentially less reliable because of the marine reservoir effect (Heaton et al. 2020). Lastly, organic matter, if not composed of (older) residual plant remains but of



Fig. 1. Location of the site Puntone Nuovo 2016.



relatively labile, short-lived organic compounds inherited from the lagoonal sediment or formed in a brine, might provide an independent check on the radiocarbon age of the precipitates and shells. This led us to attempt to radiocarbon date these three types of materials – precipitated ‘secondary carbonates’, shells and organic matter – from several strata in and near the brine pit, representing various stages in the salt industry at the Puntone site.

Evidently, information on the potentially complex origin of the materials is crucial for a proper interpretation of the radiocarbon dates (Douka et al., 2010; Pigati, 2013). For example, secondary carbonates encountered might be partially composed of recent pedogenic carbonates and of older detrital (primary) carbonates, and part of the organic matter might be of recent age, such as roots from recent trees. To obtain the required information, we performed a range of analyses, which form the core of the first topic of this paper: the origin of these materials – secondary carbonates, shells and organic matter – and their radiocarbon dating. The second topic concerns the implications of the results for the history of the briquetage site and for the temporal relations between briquetage and saltern-based production of salt in the Tyrrhenian coastal area of Central Italy.

## 2. Materials

The Puntone site, at a few meters above sea level, is located on the lower slope of a Pleistocene alluvial fan complex, which is composed of poorly sorted sediment originating from an adjacent sandstone ridge (Colle Spedaletto, see Fig. 1). The fan complex is locally covered by Holocene fluvial sediments and at sea level dips underneath Holocene lagoonal sediments. This lagoon had a natural open connection with the sea until recently (e.g., Cappuccini, 2011; Giroladini, 2012). The sandstone forms part of the Tertiary Macigno formation and is a grey to bluish-grey, well-consolidated, poorly to moderately sorted siliciclastic sandstone, classified as a greywacke. It contains some calcium carbonate (generally < 5%), while it contains in the order of 4–7%  $\text{Fe}_2\text{O}_3$  (Deneke & Günther, 1981; Dinelli et al., 1999; Cornamusini, 2002). Its Sr isotopic composition has been studied by Boschetti et al. (2005) and Nisi et al. (2008).

The pit depicted in Fig. 4 is exemplary for the pits found at the site (see Fig. 2a). It has been dug in a strongly developed and deeply decalcified paleosol with a thick reddish-brown clayey argic B horizon, which is characteristic of the alluvial fan complex. Greyish quartzitic



**Fig. 2.** a) Geophysical survey (above) with interpretation of features. Excavated areas are indicated by capital letters; b) Features studied and excavation areas: 1 = dump of fragments of briquetage vessels; 2 = infilled pits in excavated area B; 3 = geomagnetic map of excavated areas B and C with the infilled pit studied (feature B1).

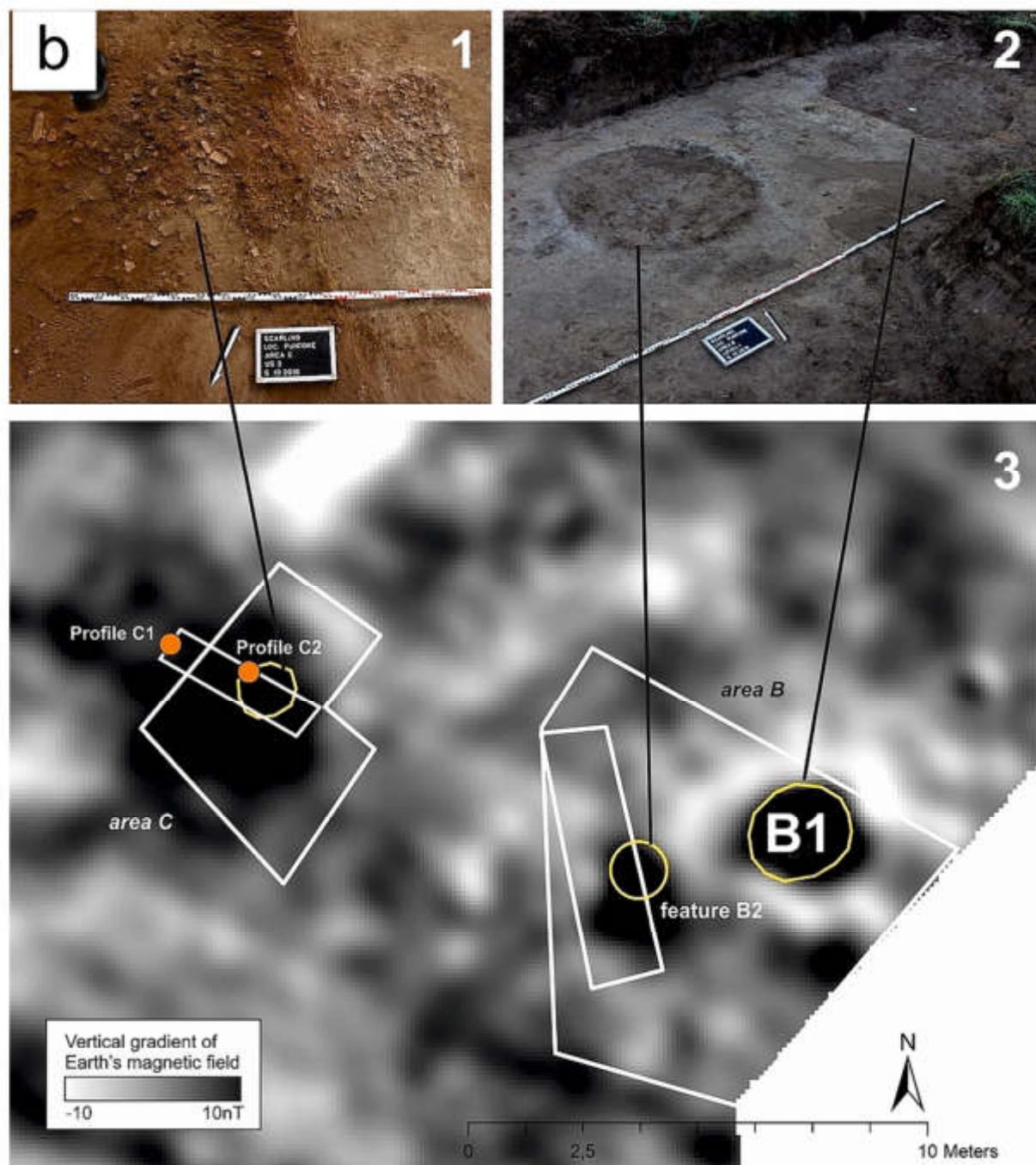


Fig. 2. (continued).

loamy sands, holding variable amounts of carbonates and consisting of leached and sieved fine lagoonal sediments, dominate the pit fill and associated strata. The carbonates were predominantly non-biogenic carbonates, but some were shells and shell fragments either as loose particles or embedded in aggregates. For a detailed description of the site, phases and various deposits, reference is made to [Sevink et al. \(2021\)](#).

### 3. Methods

The circular pit B2 and its surrounding strata (Figs. 2b and 4) were described and sampled per stratigraphic unit. Sample numbers refer to the units indicated in Fig. 4a. Various analyses were performed on untreated samples and samples that were pretreated to remove specific

compounds. Mineral fractions (2000–105  $\mu\text{m}$ ) were studied by optical microscopy and were used for hand-picking specific materials. Concise descriptions of the other analytical methods and their aims are given below. For a full overview, reference is made to supplement 1.

#### 3.1. Chemical analyses

The analyses were aimed to establish the chemical composition of the carbonate fractions and the carbonate and organic matter contents.

- Extraction with 0.25 M acetic acid (HAc) and 1 M hydrochloric acid (HCl). Weight losses were established and HCl extracts were analyzed for Ca, Fe, and Mg, using ICP-OES. These analyses served to distinguish between readily soluble (HAc) and poorly soluble



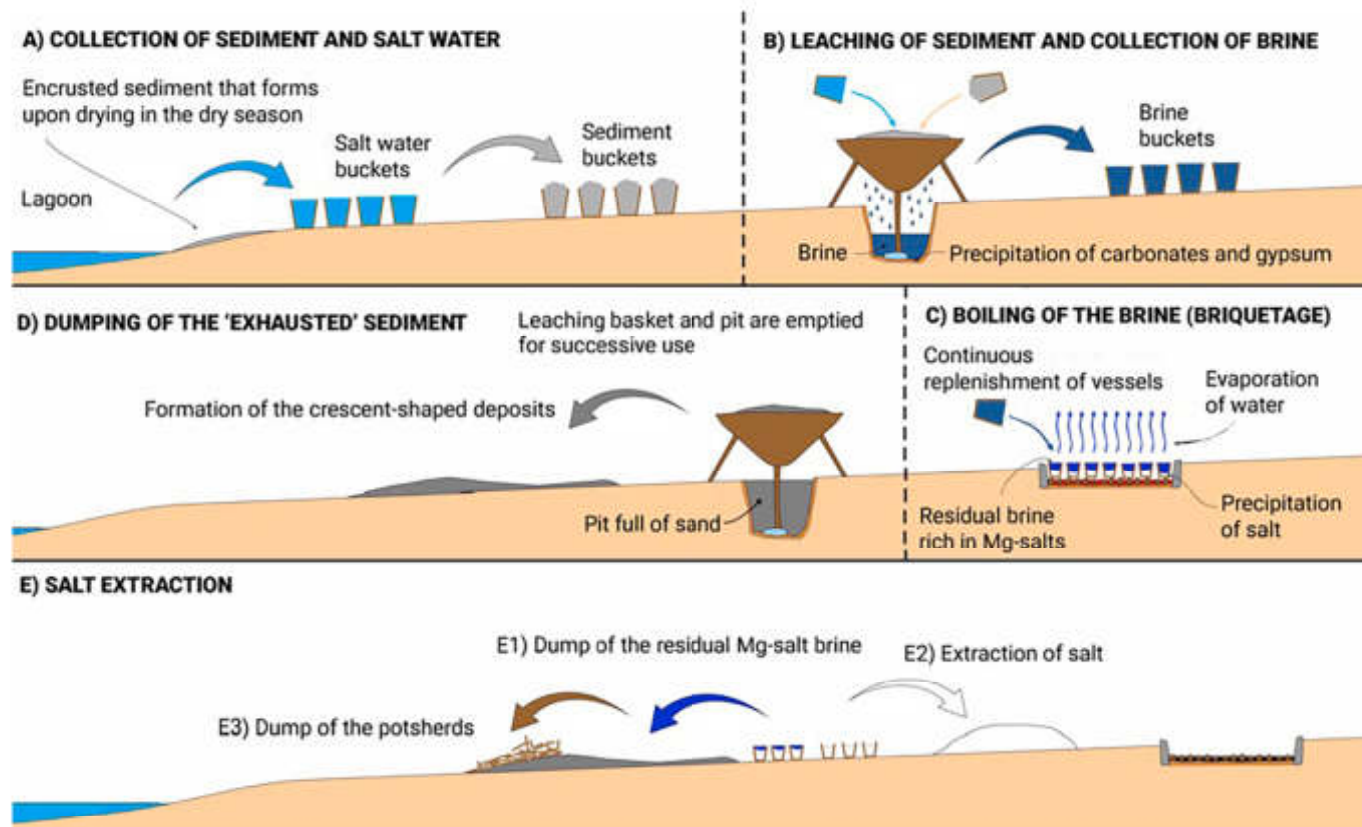


Fig. 3. The salt production processes at Puntone (from Sevink et al., 2021).

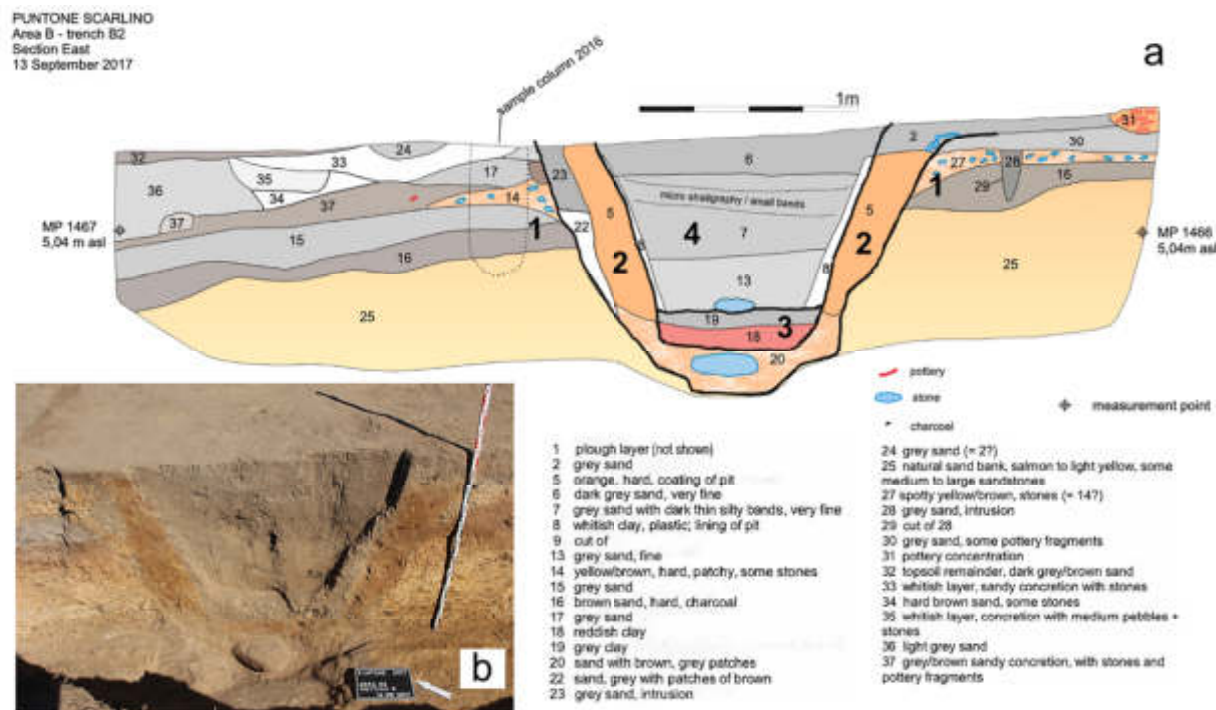


Fig. 4. a) Cross section of infilled pit with stratigraphic units (small numbers) and phases distinguished (bold numbers), modified version of original cross section from Sevink et al. (2021); b) Photograph of the pit section.

carbonates (HCl-HAc) (Raisbeck, 1999). In the carbonate-free residues from the HCl extraction C, N, and S contents were determined by an elemental analyzer.

- X-ray microanalysis and electron microscopy analysis (SEM/EDS) of secondary carbonate aggregates obtained by hand-picking from the 2000–105  $\mu\text{m}$  mineral fractions. Analyses were performed at the Osservatorio Vesuviano, Istituto Nazionale di Geofisica e Vulcanologia, Naples, Italy, using polished sections of aggregates embedded in resin and coated by rod graphite. The instrument is a SIGMA field emission scanning electron microscope by ZEISS, equipped with an XMAN micro-analysis system by Oxford, controlled by SMARTSEM 5.09 and AZTEC 3.0 softwares. Aggregates from units 13 and 19 were chosen, being representative for units that were high and low in HCl extractable iron, respectively.

### 3.2. X-ray diffraction analysis

The aim was to assess the nature of the carbonates in fine earth fractions from representative fill units and to obtain information on the overall mineral composition of these units. Analyses were performed by X-ray powder diffraction (XRD) using an X'Pert Powder diffractometer by PANalytical, at the Istituto Nazionale di Geofisica e Vulcanologia-Osservatorio Vesuviano (Napoli). The diffractometer was equipped with a high-speed PIXcel detector, Ni-filtered,  $\text{CuK}\alpha$  radiation, and pyrolytic graphite crystal monochromator, and was operated at 40 kV and 40 mA in a  $3\text{--}70^\circ$   $2\theta$  range with  $0.02^\circ$  steps at 8 s/step. Diffraction patterns were interpreted using the HighScore Plus software and JCPDS PDF-2 database.

### 3.3. Sr isotope analysis

The aim was to establish the provenance of the Sr (marine or Macigno-derived) in the carbonates (see 5.2). Compositions of hand-picked marine shells (biogenic carbonates) and aggregates of secondary carbonates (2000–105  $\mu\text{m}$  mineral fractions), as well as of fine earth fractions (PU35 and PU36) were determined by Thermal Ionization Mass Spectrometry at the Istituto Nazionale di Geofisica e Vulcanologia at Napoli (Italy), using a ThermoFinnigan Triton TI multi-collector mass spectrometer. Sr was separated by standard column chromatographic methods using the Dowex AG50WX-8 (200–400mesh) resin (Arienzo et al. 2013).

### 3.4. Microbial community analysis

DNA analyses served to establish the former microbial communities in the major pit fill units, and to derive information on the environmental conditions during their formation. DNA was extracted using the Qiagen DNeasy PowerSoil Kit (Qiagen GmbH, Germany) as described by the manufacturer. Subsequently, 16S rRNA genes were amplified with primers 341F-785R (Klindworth et al., 2013; Thijs et al., 2017) and the amplicons were sequenced on an Illumina MiSeq system by the commercial company MR DNA (Shallowater, Texas, USA). The sequences were first analyzed in SILVAngs (<https://ngs.arb-silva.de/silvangs/>) using SILVA SSU Ref dataset 132 at 97% similarity. Subsequently, the results were analyzed with MicrobiomeAnalyst (Chong et al., 2020; <http://www.microbiomeanalyst.ca/>). Data were rarefied to the minimum library size. Cluster analysis was performed using the Bray-Curtis index and Ward clustering algorithm. Some of the 16S rRNA gene sequences were aligned to sequences in the SILVA SSU Ref dataset 132 with SINA (Pruesse et al., 2012), and imported into ARB (Ludwig et al., 2004) to determine the phylogenetic position of the community members.

### 3.5. C isotope analysis

Initial carbon isotope analyses were conducted on fine earth fractions, providing data on the 'total carbonates'. This was followed by the

analysis of 'poorly soluble carbonates' in fine earth fractions (samples pretreated with HAc to remove 'readily soluble carbonates'), and of secondary carbonate aggregates, charcoal, and shells that were hand-picked from 2000 to 105  $\mu\text{m}$  mineral fractions. Since the organic matter contents of the fine earth fractions were found to be very low (expressed as organic C), we used carbonate-free  $< 63 \mu\text{m}$  fractions for the carbon isotope analysis of organic matter to ensure that samples held sufficient carbon. Samples were analyzed by AMS at the Centre for Isotope Research (CIO) of the University of Groningen. For an extensive description of the methods and AMS systems (GrA and GrM) used at CIO, see Dee et al. (2020).

$^{14}\text{C}$  dates given (in yr BP) are based on the standardized calculations, including correction for isotopic fractionation (Mook & Van der Plicht, 1999; van der Plicht & Hogg, 2006). The dates were calibrated using the software OxCal 4.4 (Bronk Ramsey, 2020) against the IntCal20 and Marine20 curves (Reimer et al., 2020; Heaton et al., 2020). The  $\Delta R$  ( $-127 \pm 28$ ) was calculated using the Marine Reservoir Correction Database (<http://calib.org/marine/>) and is the result of an average of estimated values for two nearest by sites (Naples: Siani et al., 2000; Liguro-Provençal Basin: Tisnérat-Laborde et al., 2013). All date ranges are given to 95% probability.

## 4. Results

In Fig. 4, an overview is given of the various units and phases (bold numerals) encountered in and associated with the pit. Greyish quartzitic loamy sands that in the field could be identified as processed lagoonal sediment are indicated in light greyish colors in Fig. 4a. Inside the pit, they included units 2, 6, 7, 13, 19, 22, and 23. Units 5, 18 and 20 consisted of the same quartzitic loamy sands to clay loams, but showed more or less prominent iron-staining (see Fig. 4b), brought about by gleying that occurred during phase 3, i.e. following on the 'cleaning' of the pit that existed in phase 2 and contemporaneous with the accumulation of the units 18 and 19 that accumulated in phase 3 (Sevink et al., 2021). None of the units of processed lagoonal sediment contained more than a trace of (gravel-sized) material that after gentle crushing did not pass the 2 mm mesh sieve. This material consisted of slightly harder aggregates of secondary carbonates. Units 8 represented the clay 'plaster' of the pit wall. Units 14, 16, 27 and 37 consisted of reworked paleosol material, often with some admixture of gravel and stones, derived from Macigno sandstone, and in unit 16 some charcoal. The paleosol in the alluvial fan material is marked as unit 25. Further materials studied include samples from this paleosol, taken at 1 m upslope from the pit (samples PU35 and 36) and soft carbonate incrustations (PU8) on briquetage pottery fragments from an intercalated stratum in a nearby dump of processed lagoonal sediment (see Sevink et al., 2021). Results are briefly described to facilitate the general discussion, which is focused on the origin of the various materials and their radiocarbon dating.

### 4.1. Chemical and mineralogical analyses

#### 4.1.1. Microscopic observations

Microscopic study of the 2000–105  $\mu\text{m}$  mineral fractions from the quartzitic loamy sands showed that they are composed of quartz and lesser amounts of secondary carbonate aggregates, feldspars, and micas (muscovite and some biotite). Overall, the aggregates are small and composed of micro-crystalline secondary carbonates (non-biogenic) with some embedded non-carbonate fine mineral grains (quartz, mica etc.). Samples 6, 7, and 13 additionally held a few percent of small (mostly  $< 1 \text{ mm}$ ) marine shells and shell fragments (see Figs. 5 and 6b), as loose material and as embedded material in the secondary carbonate aggregates. Other samples from the greyish quartzitic loamy sands contained at most traces of biogenic carbonates (shells). For the species composition of the shells reference is made to Sevink et al. (2021).

Shells found in the samples from units 6, 7 and 13 included extremely well preserved and fragile millimeter-size juvenile individuals, lacking



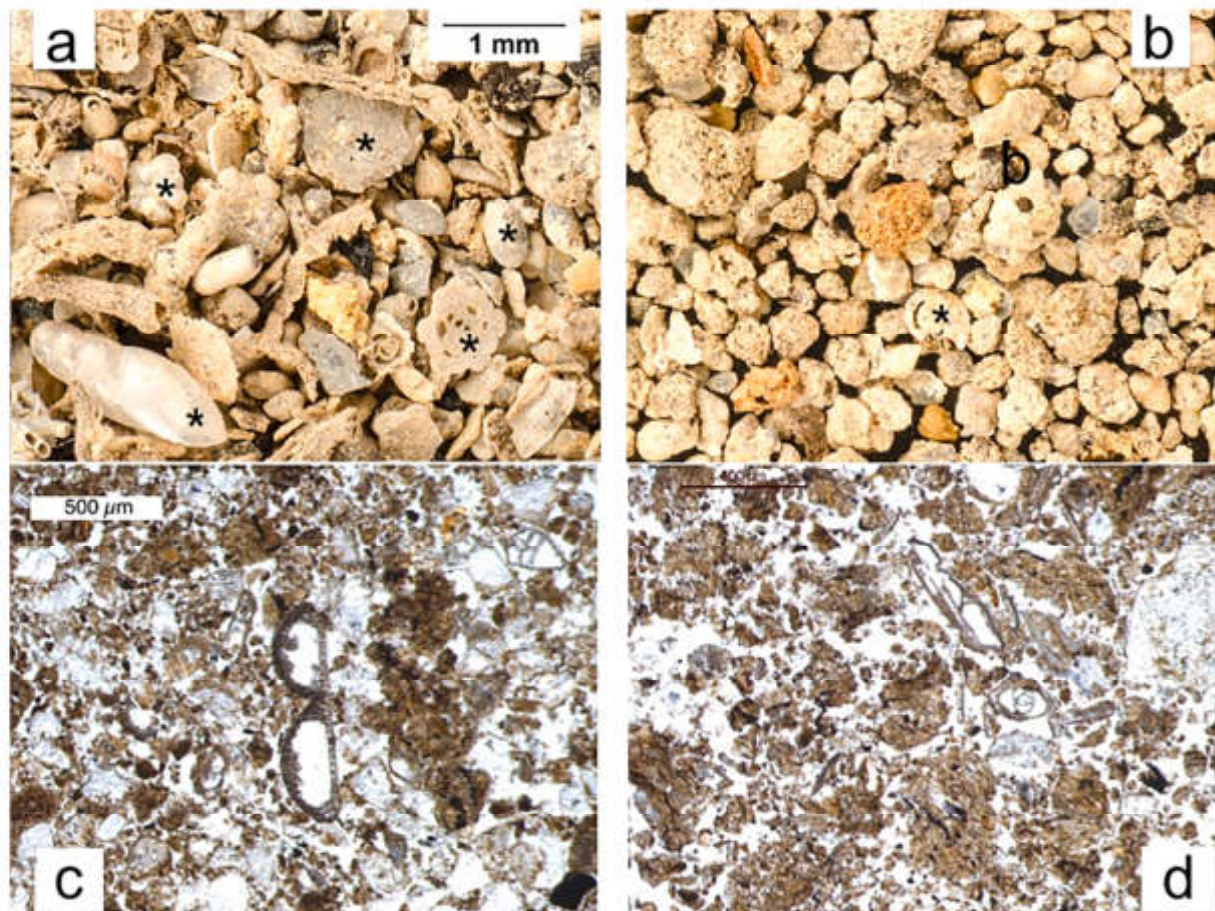


**Fig. 5.** Fractions  $> 63 \mu\text{m}$  (a and b) and thin sections (c and d): a) Unit 6 with common fossils, some of which are indicated with \*; b) Unit 13 with some fossils (\*); c) and d): Thin sections of unit 7, both with extremely well preserved shells.

any trace of weathering. The complete absence of traces of dissolution was confirmed by observations in a thin section of unit 7 (see Fig. 5c and d). Shell fragments were also found in the SEM/EDS sections, particularly in unit 13 (see Fig. 6b). Their preservation and eventual dissolution could not be judged from these sections. Secondary carbonates were either rhombuses and up to  $10\text{--}30 \mu\text{m}$  in size, or irregular in shape and of smaller size; each type clustering in different areas (Fig. 6c–e). Samples from reworked paleosol material and the paleosol itself typically consisted of quartz, feldspars and micas (both muscovite and biotite), with additional more or less weathered composite lithic fragments (weathered greywacke). Accessory materials included iron-manganese aggregates, very minor amounts of ceramic fragments and, in sample 16, charcoal.

#### 4.1.2. X-ray diffraction analyses (XRD)

Results from the analyses are listed in Table 1 and provide a rough indication for the bulk compositions. For the diffractograms and details on the reliability of the data, reference is made to Supplement 3. In processed lagoonal sediment (6, 13, and 19), the mineral assemblages mainly consisted of carbonates, followed by quartz and feldspars. Contents of micaceous minerals were small but in sample 13 a relatively large amount of mica was found. Sample 8 (clay plaster from the pit) and the paleosol samples (PU35 and PU36) were fairly high in micaceous minerals. The paleosol materials contained illite, mica, and vermiculite, in addition to feldspars, whereas the plaster was fairly high in illite and calcite, the latter being absent in the paleosol material. Quartz was detected in all samples, with relatively low contents in samples 13 and 19. Carbonate contents of processed lagoonal sediment were high (over 50%), with a mixture of ankerite and calcite in sample 6, and solely calcite in samples 13 and 19.

#### 4.1.3. Chemical analyses

Results from the extraction with HAc and HCl, and subsequent analysis of the residues for C, N, and S are presented in Table 2 (for full analytical data, see Supplement 2). Percentages of Fe, Ca, and Mg pertain to their relative concentrations in the HCl extracts. The solubility of iron minerals such as goethite, hematite, and magnetite in cold 1 M HCl is low and the same holds for iron-bearing silicates (Raiswell et al., 1994). Some dissolution of other Fe-holding non-carbonate minerals may have occurred, such as poorly crystalline iron(hydr)oxides. As to the abundance of such iron compounds, the colors of the materials analyzed – greyish to light creamy – were such that their contents of iron (hydr)oxides must be very low ( $<1\%$   $\text{Fe}_2\text{O}_3$ ; see e.g., Schwertmann, 1993). Therefore, the bulk of the extracted iron must have been present as carbonate. Assuming that  $(\text{Fe} + \text{Ca} + \text{Mg})$  forms c. 45 wt% of the total carbonate fraction (the remainder being  $\text{CO}_3$ ) and that the weight losses result from dissolution of carbonates, weight percentages of Fe and Mg in the form of carbonates would be 1.2–2.8% Fe and 1.0–4.2% Mg, respectively (see Table 2).

Given the known differences in solubility between various types of carbonates (see Rallsback, 1999), the ‘readily soluble carbonates’ (HAc extraction) will stand for the rather pure (low Mg and/or Fe) calcium carbonates aragonite (‘shell carbonates’) and high calcium calcite, while the ‘poorly soluble carbonates’ most probably stand for calcites that are relatively high in ferrous iron and/or magnesium, as well as for ankerite. The analyses pertain to the overall chemical composition of the carbonates, implying that they may well consist of a mixture of chemically quite varied types of carbonates.

The SEM/EDS analyses concern hand-picked large secondary carbonate aggregates (fraction  $2000\text{--}105 \mu\text{m}$ ) from the units 13 and 19, representing units that differ in extractable Fe and Mg contents (see



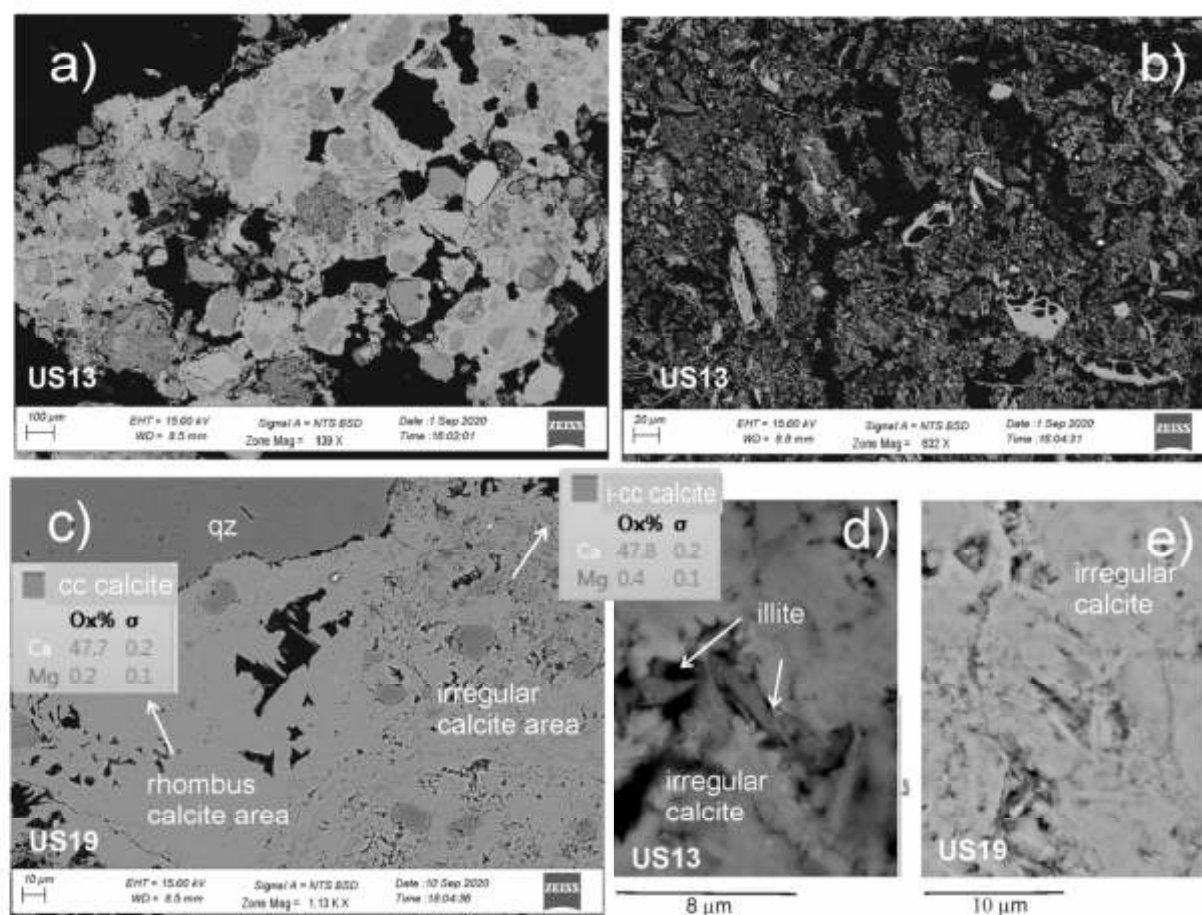


**Fig. 6.** SEM data and EDS results for samples from units 13 (US13) and 19 (US19): a) Micritic calcite; b) Fossils; c) Two types of calcite and their chemical analyses; d) and e) Irregular calcite.

**Table 1**

XRD results in estimated weight % of the various minerals.

Sample	Illite	Mica	Vermiculite	Calcite	Ankerite	Feldspars	Quartz
8	22.7	2.3	–	29.0	–	8.8	37.2
PU35	17.6	8.0	6.4	–	–	39.0	29.0
PU36	3.4	16.9	8.4	–	–	40.6	27.7
6	–	0.6	–	38.7	20.6	9.8	30.3
13	1.2	26.1	–	52.6	–	6.5	13.6
19	1.3	0.2	–	73.5	–	11.0	14.0

The refining procedure accuracy was based on the agreement indices listed in the Table S1. The error is in the range of  $\pm 0.5$ .

**Table 2**

Readily dissolved (HAc) and Total carbonates (HCl); chemical composition of the carbonates expressed as Sum of Fe + Ca + Mg = 100%; weight percentage of element presumable present as carbonate in the fine earth fraction; C, N, and S content of carbonate-free residues.

Unit US	Carbonates HAc (%)	Carbonates HCl (%)	(Fe + Ca + Mg) in carbonates = 100%			Element as carbonate in % < 2 mm fraction			Carbonate-free residue			
			Fe [%]	Ca [%]	Mg [%]	Fe%	Ca%	Mg%	C %	N%	S%	C/N ratio
6	1.41	32.0	16	55	29	2.3	7.9	4.2	0.79	0.039	0.031	20
7	1.71	36.1	12	65	24	2.0	10.6	3.9	1.63	0.081	0.049	20
13	0.69	31.9	16	66	21	2.3	9.5	3.0	1.41	0.083	0.051	17
19	3.93	28.2	22	70	8	2.8	8.9	1.0	0.54	0.050	0.022	11
20	2.38	15.4	17	68	15	1.2	4.7	1.0	0.27	0.030	0.022	9
15a	1.57	22.7	18	65	17	1.8	6.6	1.7	0.29	0.010	0.014	29
15b	1.55	29.3	16	65	18	2.1	8.6	2.4	0.46	0.020	0.015	23
17	1.63	23.5	24	59	17	2.5	6.2	1.8	0.14	0.010	0.013	14



**Table 2).** Extensive analytical results and backscattered images can be found in supplement 5, while here overall trends and results are presented. The main mineral phases were quartz, calcite (both biogenic and non-biogenic), plagioclase (oligoclase and albite), and K-feldspar, and minor amounts of micaceous minerals (mainly mica and fine-grained illite). The non-biogenic (secondary) calcite generally contains some Mg, with higher values in sample 13. Moreover, two types of non-biogenic calcite were observed: rhombic calcite with lower Mg content and irregular aggregates with higher Mg contents (see Fig. 6c). Differences between these types of calcium carbonates are not limited to the Mg content: the rhombic form is a relatively pure calcite, while the aggregates in addition to Mg contain some Fe, and often also some Si and Al, as well as fine micaceous mineral fragments.

Whether Mg and Fe form a structural component of the fine micaceous minerals included in the aggregates or of the carbonates is not fully clear from the point data. These exhibit rather erratic ratios between Mg, Al, Si, and Fe, with Al/Si ratios being especially variable (see supplement 1.2). Moreover, as is evident from the spatial distribution of the various elements (see supplement 1.3), there is no truly systematic spatial correlation between concentrations of Al and Si, on the one hand, and those of Fe and Mg on the other hand, implying that some Fe and Mg might be present as a structural component of non-biogenic (secondary) calcite. Some calcite is indeed relatively high in Fe as demonstrated by Fig. 7. In this context, it is interesting to note that in our EDS sections Fe is mostly found in submicron-sized particles (see Figs. 7 and 8, and, for details, supplement 1.3) and that Xu et al. (2019) demonstrated that submicron-sized microbial ferroan carbonates can be formed in environments that in terms of their microbial communities very strongly resemble those that we studied.

As to the carbon content of the HCl extraction residues, the values in Table 2 demonstrate the low organic matter content of the various materials, which with regard to their C/N ratio vary considerably, with lowest values for samples 19 and 20. Carbon contents of the fractions < 63 µm are distinctly higher (see Table 3), demonstrating that most of the organic matter is concentrated in the finer fraction.

#### 4.1.4. Summary remarks

Differences between carbonate contents established by XRD (Table 1) and by extraction with HCl (Table 2) are evident. These are attributed to the fact that the two analyses were performed on different aliquots, and those used for the XRD analyses were not representative of the bulk (fine earth fractions). Differences between the SEM/EDS and XRD results are quantitative (particularly amounts of micaceous minerals). Furthermore, in the SEM/EDS analyses carbonates are generally low in Fe and Mg, whereas higher Fe and Mg concentrations were encountered in the fine earth fractions (HCl extracts). This suggests that significant differences exist between the composition of the large secondary carbonate aggregates and those of the much finer carbonate aggregates in the fine earth fractions (loamy fine sand) comprising predominantly fine sand to silt-sized particles.

#### 4.2. Sr isotopic analyses

In Fig. 9, the results are presented, while details are given in supplement 4. Samples 6 and 7 shells and carbonate, 13 shells, and 19 have Sr isotopic ratios that are similar (within the analytical error) and virtually identical to those of seawater (c. 0.7092). The secondary carbonates from units 13 exhibit a significantly higher value (c. 0.7094).

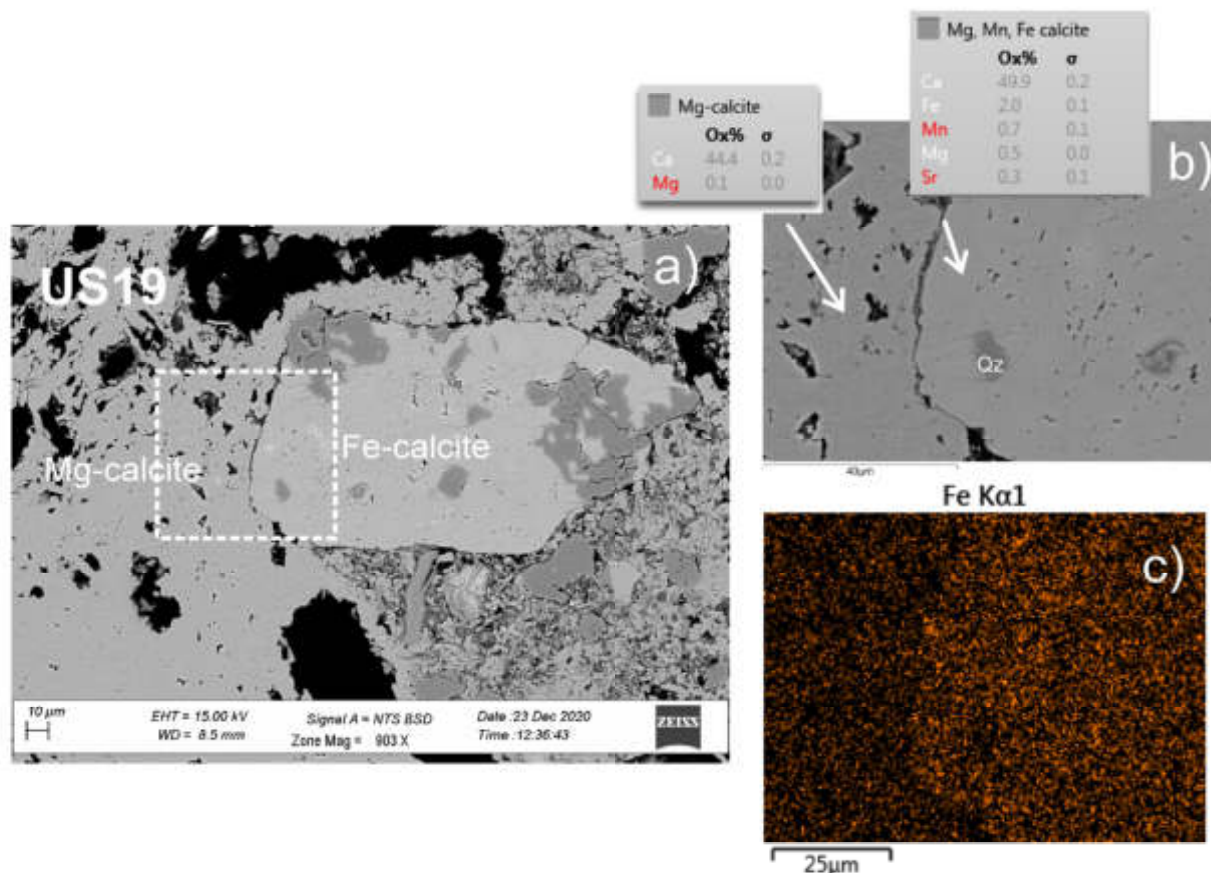


**Fig. 7.** SEM data and EDS results for samples from unit 19 (US19): a) EDS scan with 2 types of calcite, b) Chemical analyses for these calcites, and c) Distribution of Fe.

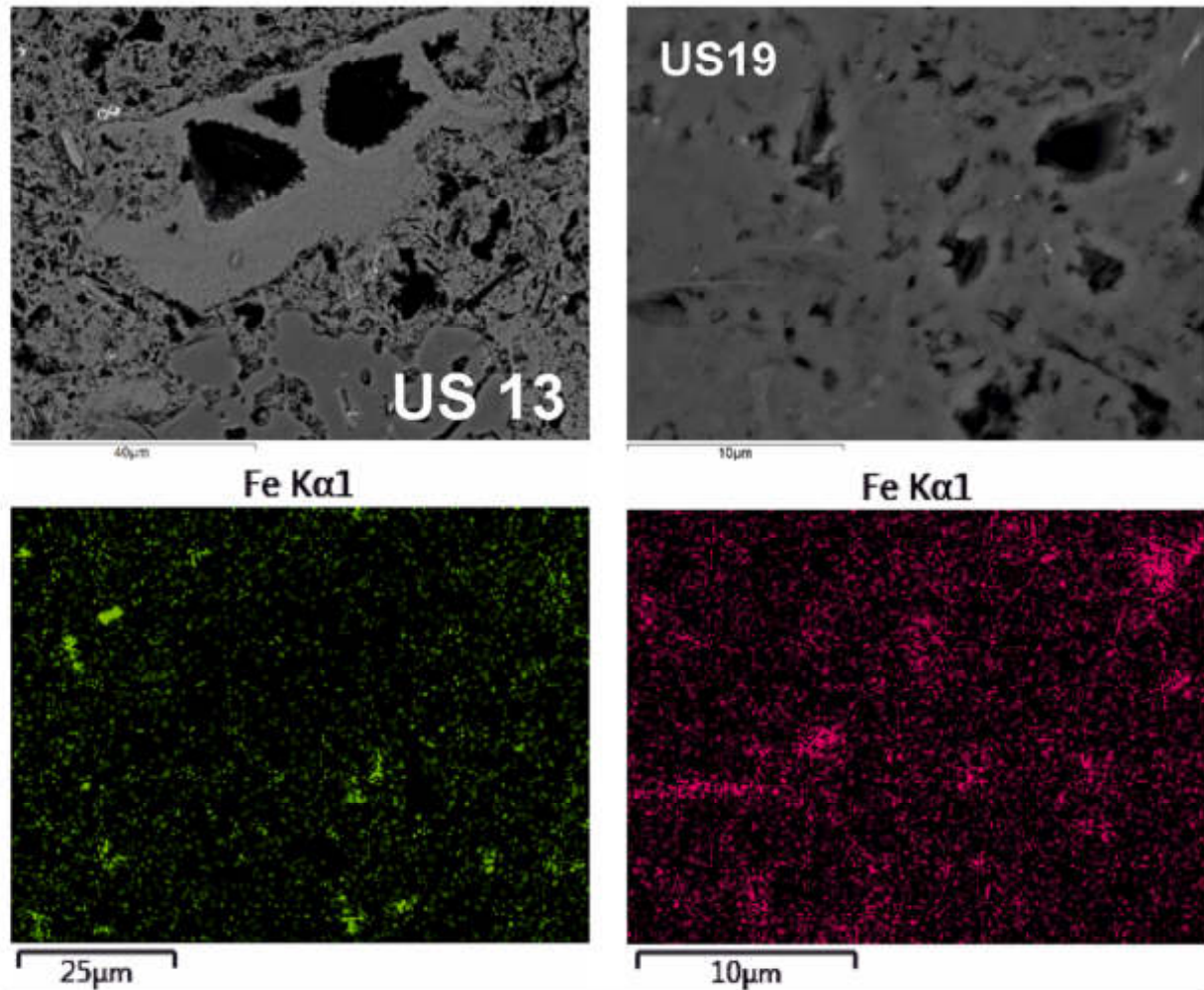


Fig. 8. EDS scans and distribution of Fe in these scans for unit 13 (US13) and 19 (US19).

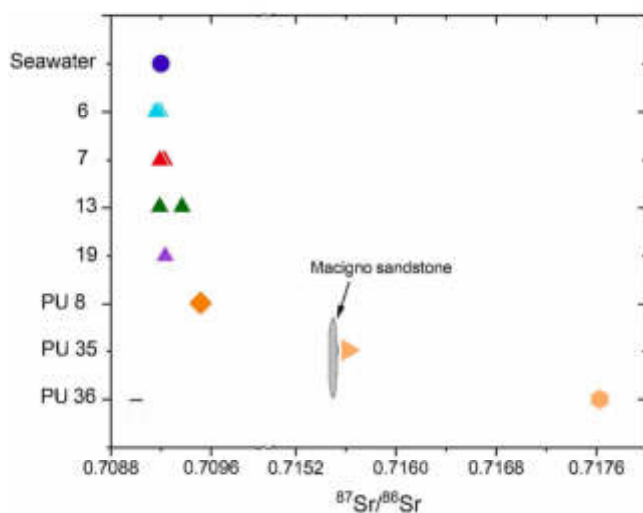


Fig. 9. Sr isotopic ratios for secondary carbonates in the various samples and reference values for Macigno sandstone and seawater.

The same holds for sample PU8, which consists of secondary carbonate encrustations on ceramic fragments having a value of c. 0.7095, and for the samples PU35 and PU36 that both are from the paleosol in Macigno-derived fan deposits (c. 0.7156 and 0.7176, respectively).

Sr isotopic ratios of the Macigno sandstone, the dominant rock type in the area and the only sediment source for the non-marine/lagoonal Quaternary sediments, are significantly higher than that of seawater (c. 0.7155; Boschetti et al., 2005; Nisi et al., 2008), suggesting that sediment derived from this sandstone was the source of the Sr for the secondary carbonates with higher isotopic ratios. The Sr will have been released by weathering of the Macigno derived material, which most probably is also responsible for the relatively elevated Fe contents of the secondary carbonates. These conclusions regarding the origin of the Sr isotopes are in line with the results of the study by Pennisi et al. (2006) on the nearby Cornia Plain, who found seawater-type Sr isotopic ratios in groundwaters and sediment leachates from coastal sediments with relatively high Cl concentrations and conductivities.

#### 4.3. Microbial community analyses

16S rRNA gene amplicon sequencing of the microbial DNA showed a dominance of Proteobacteria (38%) and Actinobacteria (26%) in all samples as well as several phyla that were less abundant, such as the Acidobacteria (10%), Chloroflexi (7%), Gemmatimonadetes (4%), Bacteroidetes (3%), and Planctomycetes (2%) (Fig. 10). Proteobacteria were mainly represented by Gammaproteobacteria (22%), followed by Alphaproteobacteria (12%) and Deltaproteobacteria (4%). Archaea, i.e., Euryarchaeota, were only found in sample 13. The overall composition of the microbial communities in our samples, in particular the dominance of Gammaproteobacteria and the absence of Betaproteobacteria, is similar to that of microbial communities found in marine sediments



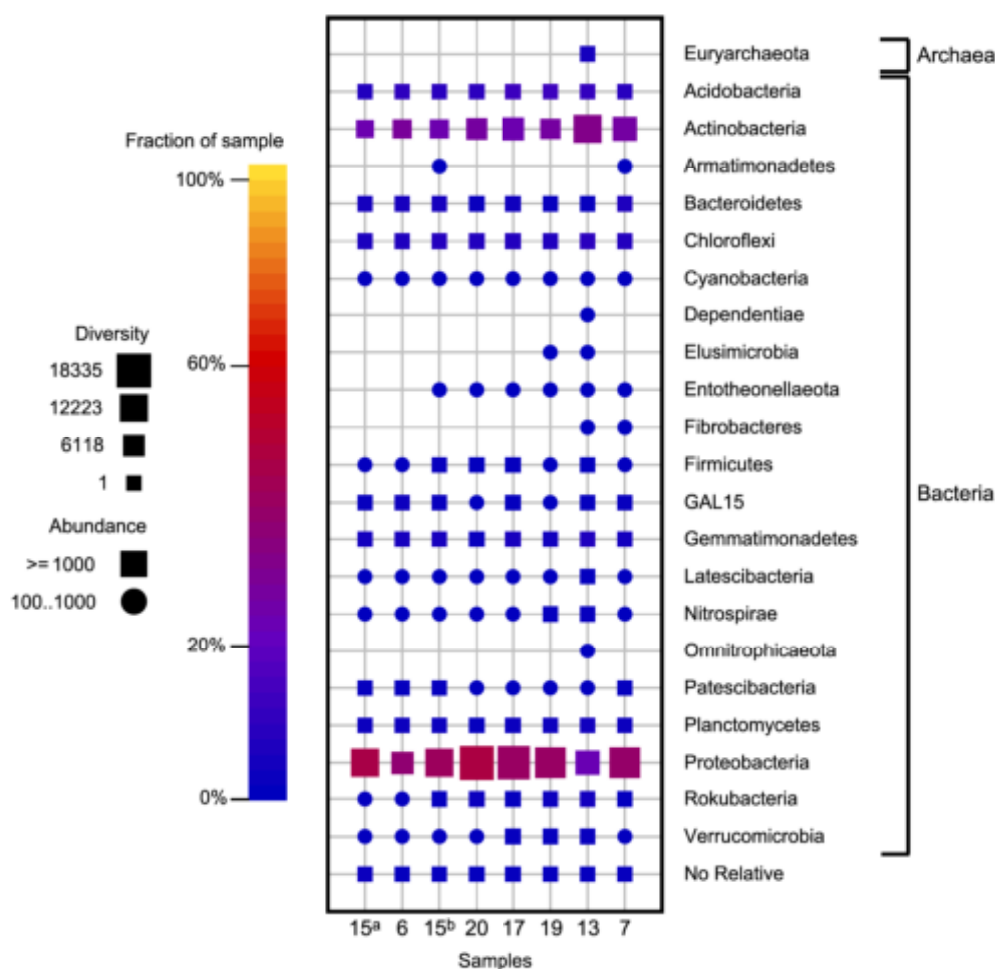


**Fig. 10.** Taxonomic fingerprint at the phylum level of microbial communities. The size of the symbols is scaled to the number of sequences found per OTU. Colors indicate the fraction of a dataset that an OUT represents. Circles and squares indicate the dominance of the OTU; OTUs with <100 reads were excluded.

(see figure 20.36 in Madigan et al., 2019) and, more specifically, in Mediterranean coastal systems such as the Camargue (Osman et al., 2019). They testify to the marine origin of these materials, but additionally exhibit clear variation in composition as evidenced by the cluster analysis of the 16S Amplicon sequences (see Fig. 11).

This cluster analysis shows that communities in the units 15a, 15b, and 17, all of which are from the earliest phase (phase 1), are very similar and differ from those of more recent units, though differences with those of units 6 and 7 are limited. Communities of units 19 and 20 form a separate cluster. They are from the lower part of the pit but are from different pit fill phases (2 and 3). Units 6, 7 and 13 are from the latest phase (phase 4). Unit 13, which is the lowest unit from this phase, differs strongly from all other communities. The observed similarity between the communities in units 6, 7, 15 (a and b), and 17 thus indicates that the microbial DNA in these materials primarily originates from the sediment that was taken from the lagoon and can be linked to the conditions in this lagoon. The limited variation in their composition is in line with observations of the temporal variation in microbial communities for Mediterranean lagoonal flats (see e.g., Osman et al., 2019). Consequently, the distinctly deviating composition of the communities in units 13, 19, and 20 indicates that they reflect conditions in the pit and their temporal variations. Additional arguments may be found in the presence of bacteria that are very unlikely to have existed in the surficial sediments of the seasonally desiccated lagoonal flats.

Phylogenetic analysis of the most dominant sequences of the Archaea in unit 13 shows an affiliation with the methanogen

*Methanomassiliicoccus luminyensis*. In the same sample sequences occur that are related to the methanotroph *Candidatus methylomirabilis oxyfera*, a bacterium that can oxidize methane with nitrite as an electron donor. Both species are strict anaerobes (Dridi et al., 2012; Ettwig et al., 2010) and thus indicative of prominently anoxic conditions as may have existed in the lower part of the pit during phase 4. In the units 6 and 7 from the same phase, these species were not observed, nor were they found in the other units, which provides a strong support for the non-existence of such conditions in the seasonally dry lagoon from which the sediment was taken. The presence of certain microbial groups, such as the Patescibacteria and Latescibacteria that grow by fermentation of polysaccharides and glycoproteins (Youssef et al., 2015; Beam et al., 2020; Tian et al., 2020), and the dominance of the Dehalococcoidia (phylum Chloroflexi), suggests that overall - both in the lagoon and in the pit - more or less oxygen-depleted conditions existed, though clearly less prominent than in unit 13.

As to the salinity and temperature conditions in the pit, halophilic bacteria, e.g., Halomonas, Salinispira, and Halobacter that are typical for hypersaline environments such as salterns (Osman et al., 2019) were not found. This implies that salt concentrations in the brine, standing in the pit, will not have reached such levels. The presence of members belonging to the class Thermophila might point to an elevated temperature but so far little is known about the physiology of these members, and so no firm conclusion can be drawn.

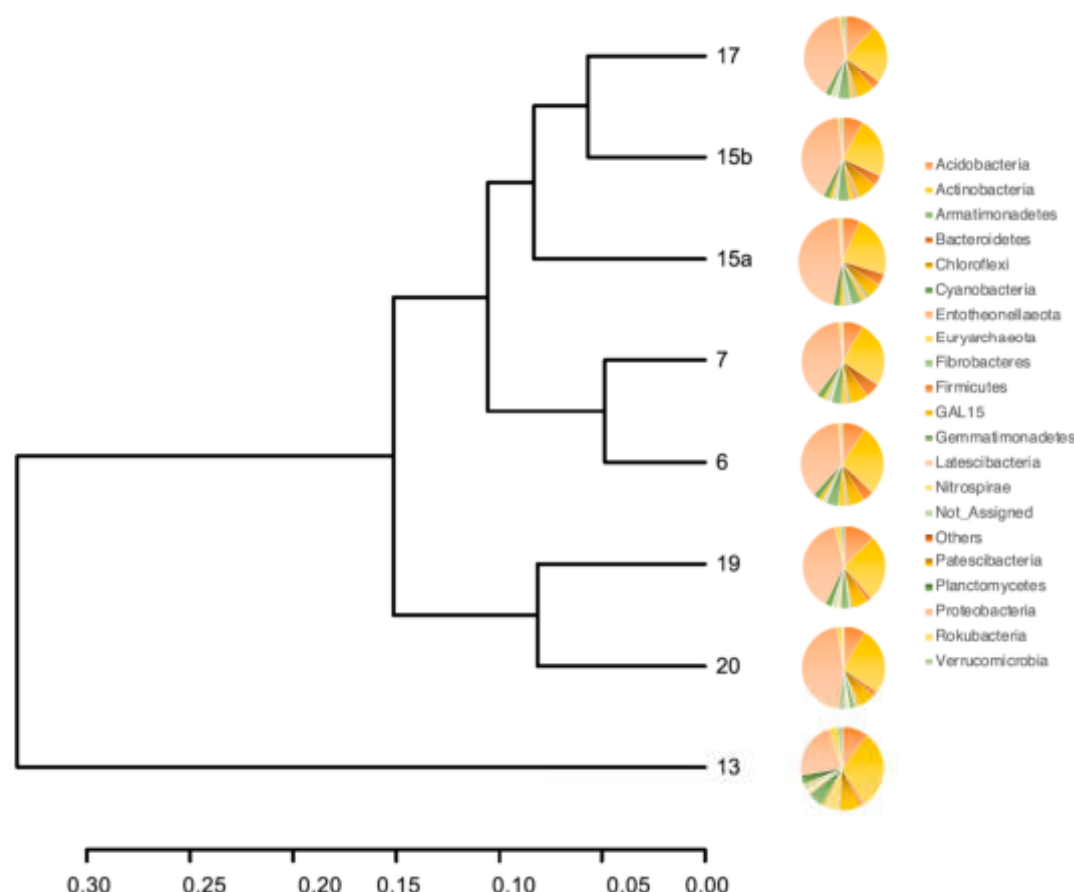


Fig. 11. Cluster analysis of the microbial communities based on 16S rRNA gene sequences at the phylum level. Bray Curtis.

#### 4.4. C isotopic analyses

In Table 3 an overview is presented of the results. Initial analyses were performed on hand-picked charcoal (2000–105  $\mu\text{m}$  mineral fractions) and on total carbonates in fine earth fractions (indicated as 'Carbonate'). This 'Carbonate' evidently may have consisted of a mixture of secondary carbonates and shell remains (biogenic carbonates), ratios between these components being uncertain. Therefore, subsequent analyses were performed on hand-picked shells ('Shells') and secondary carbonate aggregates ('Secondary Carbonates') from the 2000–105  $\mu\text{m}$  mineral fractions. Though carefully selected to indeed represent secondary carbonate aggregates, they may have held some small-sized biogenic carbonate in the form of included shells or shell fragments (see 4.1.1). In addition, samples were analyzed that were pretreated with acetic acid to remove readily soluble carbonates ('Poorly soluble - P.S. - carbonates'), assuming that this pretreatment would remove biogenic carbonates. Analyses for carbonate-free < 63  $\mu\text{m}$  fractions are indicated with 'Organic Matter'. Only in units 6, 7, and 13 (all from phase 4) adequate amounts of recognizable shells were encountered. Shells from units 6 (the youngest unit of phase 4) and 13 (the oldest unit of phase 4) were dated. Two carbonate incrustations from ceramic fragments of briquetage vessels ('Carbonates', PU8 and PU9) were analyzed, which might have been formed during the briquetage process by precipitation from the brine held in these vessels and thus eventually might be used to date the process.

#### 5. Discussion

The first aim of our research was to obtain more precise data on the age of the briquetage industry, based on the radiocarbon dating of the carbonates (shells and secondary carbonates) and organic carbon (SOM

and charcoal). The origin of these materials plays a crucial role in the interpretation of the radiocarbon data and is discussed first. This is followed by a discussion on these dates and their implications for the relation between the briquetage and saltern-based production systems.

##### 5.1. Origin of the organic matter

The stability of organic matter in lagoonal environments varies, with the labile fraction (LOM) being very easily decomposed (see below), but at a centennial time scale refractory organic matter (or ROM) is also decomposed (see e.g., Pusceddu et al. 1999). This implies that organic matter, if 'fossilized' by its burial under fresh sediment/material, is basically a suitable proxy for radiocarbon dating the corresponding sediment or stratum. Samples that are dominantly composed of LOM will provide the most reliable radiocarbon age, while those in which ROM prevails are less suitable, since these likely lead to overestimation of the age of the stratum concerned.

Few studies exist on the content and composition of organic matter in coastal sediments from Central Tuscany. The only study seems to be that by Renzi et al. (2015), who found low organic carbon contents (<1%) but provided no further information on its composition. More information is given by Renzi et al. (2019) but their study is on a shallow, stagnant and non-vegetated system in the Orbetello lagoon, in southern Tuscany, with very low redox potential in its bottom sediments. Here, total organic carbon in the upper 10 cm of the sediment amounted to <1% and it was concluded that even a limited period of exposure to oxic conditions was sufficient to change the composition of the organic matter by rapid mineralization of the labile fraction (LOM). This fraction, which was primarily of microbial origin, was found to form only a small part of the total organic matter (around 10% overall), the remainder being the stable, refractory organic fraction (ROM). Turnover



**Table 3**

Radiocarbon data for samples from the pit and dump materials. Dates for 'Shells' are calibrated against the Marine20 curve; dates for secondary carbonates from units 6, 7, 13 19 and 15a are calibrated against the IntCal20 curve and the Marine 20 ( $\Delta R = -127 \pm 28$ ) curve; all other samples are calibrated against the IntCal20 curve. All date ranges are given to 95% probability. 'OM' = Organic matter in fraction < 63  $\mu m$ , but for unit 16 the date is on charcoal; 'P.S. Carb.' = Poorly soluble carbonates; 'Sec. Carb.' = Secondary carbonate aggregates; 'Carb.' = Total carbonates in fine earth fractions. Ages for organic matter samples, dominantly composed of labile organic matter (LOM), and for charcoal, are indicated in bold (see also 5.1).

Stratigraphic unit + sample number + type	Dated fraction	Prep technique	GrA/GrM	%C	$\delta^{13}C$ (IRMS)	$\pm$	$\delta^{18}O$ (IRMS)	$\pm$	$\delta^{14}C$	$\pm$	$^{14}C$ age (yr BP)		P.S. Carb.	Sec. Carb.	Shells	$^{14}C$ age	
											OM	Carb.				IntCal20	Marine20 ( $\Delta R = -127 \pm 28$ )
US6 HCl treated	P.S. Carbonate	acid extraction	GrM 12308	3.6	-13.58	0.05			0.6988	0.0012	2879	15	2879			1121-1004 BCE	806-495 BCE
US6 carbonate aggr.	Sec. Carbonate	acid extraction	GrM 15743	4.9	-14.72	0.05	-4.91	0.07	0.7061	0.0013	2795	20		2795		1011-860 BCE	739-400 BCE
US6 fossil fraction	Shells	acid extraction	GrM 15345	10.5	-5.44	0.05	-4.11	0.07	0.7054	0.0019	2805	20			2805	1011-904 BCE	747-407 BCE
US6 HCl treated	Organic Matter	combustion	GrM 13177	5.3	-18.71	0.05			0.7665	0.0013	2137	15	2137			343-59 BCE	-
US7 fine earth	Carbonate	acid extraction	GrA 68898	3.0	-12.67	0.05			0.7341	0.0033	2485	35	2485			775-425 BCE	356-1 BCE
US7 HAc treated	P.S. Carbonate	acid extraction	GrM 12309	4.9	-12.82	0.05			0.7260	0.0013	2572	15	2572			798-770 BCE	418-107 BCE
US7 HCl treated	Organic Matter	combustion	GrM 13173	5.5	-18.84	0.05			0.7661	0.0013	2141	15	2141			344-61 BCE	-
US13 HAc treated	P.S. Carbonate	acid extraction	GrM 12312	2.6	-12.25	0.05			0.7474	0.0013	2339	15	2339			409-389 BCE	156 BCE - 173 CE
US13 carbonate aggr.	Sec. Carbonate	acid extraction	GrM 15346	5.4	-13.83	0.05	-5.28	0.07	0.7554	0.0020	2255	20		2255		391-208 BCE	48 BCE - 269 CE
US13 fossil fraction	Shells	acid extraction	GrM 15347	7.6	-6.62	0.05	-2.35	0.07	0.6873	0.0016	3010	20			3010	1380-1132 BCE	982-682 BCE
US13 HCl treated	Organic Matter	combustion	GrM 13174	3.4	-19.84	0.05			0.7432	0.0013	2384	15	2384			515-397 BCE	-
US19 HAc treated	P.S. Carbonate	acid extraction	GrM 12310	0.9	-10.62	0.05			0.8650	0.0014	1165	15	1165			772-951 CE	1137-1404 CE
US19 HCl treated	Organic Matter	combustion	GrM 13913	0.7	-27.45	0.05			0.7207	0.0020	2630	25	2630			825-778 BCE	-
US15a fine earth	Carbonate	acid extraction	GrA 68899	2.1	-9.65	0.05			0.7480	0.0034	2330	40	2330			540-212 BCE	163 BCE - 210 CE
US15a HCl treated	Organic Matter	combustion	GrM 13176	4.6	-20.82	0.05			0.7417	0.0013	2401	15	2401			538-404 BCE	-
US16	Charcoal	combustion	GrA 68773	60.5	-23.81	0.05			0.7043	0.0028	2815	35	2815			1107-841 BCE	-
PU8 fine earth	Carbonate from pottery	acid extraction	GrA 68895	3.9	-10.31	0.05			0.8483	0.0047	1320	45	1320			643-821 CE	-
PU9 fine earth	Carbonate from pottery	acid extraction	GrA 68897	4.9	-10.68	0.05			0.8538	0.0036	1270	35	1270			662-873 CE	-

rates of the ROM were not dealt with.

The coastal system that was exploited at Puntone was a truly shallow, seasonally dry lagoon flat. Our results indicate that the lagoonal sediment used as raw material was low in organic matter, and its carbon content (see Table 2) was in the same range as reported by Renzi et al. (2015, 2019). Some variation may have existed in the microbial communities of this lagoonal flat, both seasonally and spatially (see e.g., Evagelopoulos et al., 2009; Quero et al., 2017) but the brine production system (see Fig. 3) inevitably led to homogenization of the sediment and solute that passed the sieve and was 'fossilized' upon its burial by more recent material. This implies that the organic matter in the units 6, 7, 15, and 17, which in terms of the composition of their microbial communities are very similar (see 4.3), most probably reflects the 'mean composition' of that sediment. The microbial communities in the units 13, 19, and 20 clearly deviate from those in the aforementioned units, pointing to the additional presence of microbial (labile) organic matter that later on formed in the brine held in the pit (see 4.3). Our results do not allow for a true quantification of these LOM and ROM, but information can be derived from the carbon isotope analyses as LOM from marine environments is known to differ significantly from more refractory terrestrial plant-derived organic matter.

A highly relevant study is that by Vizzini & Mazzola (2003) on the stable isotopes of C and N in the various compartments, plants and animals in the Sabaudia coastal lagoon in Southern Lazio (Central Italy). They found  $\delta^{13}\text{C}$  values of c.  $-26\text{‰}$  for terrestrial organic matter, c.  $-15\text{‰}$  and c.  $-17\text{‰}$  for microphytobenthos and macroalgae, respectively, and overall values of  $-23.0 \pm 1.0\text{‰}$ . The 'dead' organic matter comprises particulate organic matter (POM, mostly from phytoplankton algae and thus 'labile' organic matter) with seasonally variable  $\delta^{13}\text{C}$  values between  $-18.2\text{‰}$  to  $-22.3\text{‰}$ , sedimentary organic matter (SOM, mostly from terrestrial origin) with values between  $-21.7\text{‰}$  and  $-23.9\text{‰}$ , and terrestrial plants (Ter) with values between  $-25.3\text{‰}$  and  $-27.1\text{‰}$ . They conclude that their results are very much in line with other Mediterranean lagoonal environments; for example, the extensive studies on the nature and origin of these various fractions in the Gulf of Lions (France) by Darnaude et al. (2004) and Harmelin-Vivien et al. (2008).

The values found for the Puntone samples thus indicate that microbial organic matter and labile particulate organic matter that is not derived from terrestrial plants form a significant component of the samples from units 6, 7, 13, and 15 with a  $\delta^{13}\text{C}$  ‰ of  $-18.7$ ,  $-18.8$ ,  $-19.8$ , and  $-20.8$ , respectively. It is because of its labile nature that we assume this organic matter to well reflect the time of burial of the material concerned. Contrary, the organic matter in unit 19 has a  $\delta^{13}\text{C}$  value of nearly  $-28\text{‰}$  and its concentration in the fraction  $< 63 \mu\text{m}$  is by far the lowest of all samples studied (see Tables 2 and 3). This strongly suggests that it largely consists of more stable detrital organic matter of terrestrial origin, which may well predate this 'time of burial'.

## 5.2. Origin of the carbonates

As stated before, the samples comprised biogenic (shells and shell fragments) and non-biogenic carbonates. The latter can be subdivided into four potential types that are relevant for radiocarbon dating:

- Type 1: Detrital carbonates originally present in the lagoonal sediment.
- Type 2: Secondary carbonates that precipitated upon the seasonal desiccation of the sediments in the lagoon.
- Type 3: Secondary carbonates that precipitated from the brine in the pit.
- Type 4: Secondary carbonates that later on formed at some depth by precipitation from infiltrated water. This type might be defined as 'pedogenic' if formed by dissolution of carbonates in the topsoil and subsequent precipitation in the subsoil.

Biogenic carbonates and non-biogenic carbonates of types 2 and 3 are potentially suitable for radiocarbon dating the briquetage industry. This is not the case for the type 4, nor for the type 1 (detrital) carbonates, both of which may be of highly variable ages. In the samples that we used for dating inevitably a mixture of various types of carbonates was present, since none of the pretreatments allowed for full separation of a single type, except for the hand-picked shells (see 4.4). Most crucial, therefore, is whether these mixed samples contained type 1 and type 4 secondary carbonates in such amounts that they would impede radiocarbon dating attempts.

An important asset of the Puntone site is that dumped processed lagoonal sediment can be compared with pit fill materials. They should have similar contents of type 1 and 2 carbonates, but fundamentally differ regarding the potential presence of type 3 secondary carbonates.

### 5.2.1. Type 1 and 2 carbonates, and biogenic carbonates.

Field observations and tests with hydrochloric acid showed that the processed sediment in the dumps overall contains a few percent of carbonates (biogenic plus types 1 and 2 non-biogenic). In contrast, carbonate contents of the pit materials are in the order of 25–30% (see Table 2), indicative of a significant presence of non-biogenic type 3/type 4 secondary carbonates. Amounts of shells found in the pit fill materials (fractions 2000–105  $\mu\text{m}$ ) were small or even negligible. Quantities in these fractions can be readily assessed, but this is far less so for the finer fractions ( $< 105 \mu\text{m}$ ). Truly small shell fragments were, for example, evident as included primary fragments in secondary carbonate aggregates in the SEM analyses (Figs. 6b and 7) but are hard to identify under the optical microscope. However, amounts of readily soluble carbonates in the fine earth fractions are low (see Section 4.1.3), suggesting that these finer fractions are also low in biogenic carbonates.

There is no modern analogue that might provide a reliable reference for the original composition of the lagoonal sediment. The reason is that the current coastal system has been heavily impacted by a massive dump of highly calcareous residues from the huge Rosignano Solvay soda ash plant at Follonica (Pranzini, 1978) and by pollution caused by other major chemical industries. Studies on the pre-industrial coastal sediments offer varied information (Gandolfi & Paganelli, 1975; Leoni and Sartori, 1996, 1997; Renzi et al., 2015, 2019; Sarti et al., 2020). Overall, these studies show that amounts of type 1 detrital carbonates ('lithic carbonate fragments') were most probably in the order of a few percent only, with shell material forming an even smaller fraction. This is very much in line with our observations on the occurrence of biogenic and type 1 carbonates. Evidently, contents of type 2 carbonates are also low, given the overall low proportion of carbonates in the processed lagoonal sediments in the dumps.

### 5.2.2. Type 3 and 4 carbonates

Clear but rather indirect evidence for the occurrence of type 3 carbonates are the differences in magnetic properties between the pit fill materials and the dumps (Sevink et al., 2021). Based on the 'wet chemical analyses' presented in Table 1, these were attributed to the formation of ferroan-magnesian carbonates (type 3) in the pit. The formation of such carbonates requires an anoxic environment and adequate supply of reduced iron, an environment that existed in the pit (see 4.3). In this context, the study by McBride & Parea (2001) on the formation of secondary carbonates in coastal sands from Tuscany is highly relevant. They demonstrated that type 4 carbonates are very high in Ca, may contain some Mg, but are free of ferrous iron. This follows from the geochemical behaviour of iron in a well-drained and aerated environment (Krauskopf, 1967; McBride, 1994): if released by weathering or present as secondary iron compounds, it occurs as ferric iron, is immobile, and thus cannot be incorporated in a calcite lattice.

The SEM/EDS analyses shed some doubt on the dominance of ferroan-magnesian carbonates since they showed that the carbonate aggregates that were analyzed (13 and 19) largely consisted of calcium carbonate, and minor amounts of Mg, while carbonates containing Fe



are relatively scarce. Reasons for the discrepancy between these results, on the one hand, and the combined results of the XRD analysis and HCl extracts have already been discussed in para 4.1.3 and are most probably related to fraction-size related differences in composition of the pit fill materials. Moreover, these SEM/EDS analyses do not provide an explanation for the specific magnetic behaviour, which is of a type matching the properties of ferroan-magnesian calcites (Sevink et al., 2021). Anyway, they indicate that some type 4 carbonates are present in the 2000–105  $\mu\text{m}$  fractions, having a chemical composition as described by McBride & Parea (2001).

As stated in Sevink et al. (2021), there is no evidence for carbonate leaching in the topsoil and subsequent accumulation of these dissolved carbonates in the subsoil, i.e. of younger type 4 carbonates. This conclusion was based on the presence in units 6, 7, and 13 of very fragile and minute juvenile shells (see 4.1.1). Further indications are provided by the carbonate contents of the various strata, which are in the order of 25–30% with some but rather minor variations in content. Such distribution is incompatible with significant decalcification (dissolution) of the upper strata, i.e. with a classic ‘pedogenic’ origin of these secondary carbonates (Duchaufour, 2012). These observations do not preclude that the lower strata at the site contain type 4 carbonates formed by precipitation from infiltrated run-off. Such run-off could have obtained dissolved carbonates from topsoils further up the slope, a process that does not necessarily require carbonate leaching in the upper strata at the briquetage site itself.

Strong indications for such a process come from the Sr isotope analyses, particularly of the carbonate encrustations on the sherds (PU8 and PU9; see 4.2 and Fig. 8). Assuming the secondary carbonates did form by dissolution of carbonates in the topsoil and subsequent precipitation deeper in the profile, they should have retained the Sr isotopic ratio of the topsoil carbonates, i.e. a ratio close to that of seawater. However, on the overlying slope of the alluvial fan, soils in Macigno-derived sediment have a distinctly higher Sr isotopic ratio. In other words, the Sr isotopic ratio lends further weight to the explanation given above for the genesis of type 4 carbonates and their occurrence, i.e. by precipitation from infiltrated lateral run-off.

$\delta^{13}\text{C}$  values might provide a clue to the origin of the carbonates, since values for carbonates in which  $\text{CO}_2$  is incorporated from decomposing terrestrial plant material should be far lower than those of marine origin. The background is that soil organic matter, which is the major source of  $\text{CO}_2$  in soils, has a  $\delta^{13}\text{C}$  value of  $-25\text{‰}$  or lower (Boutton et al., 1998). A SOM-origin thus would likely show up in the isotopic signature of ‘pedogenic type 4 carbonates’, but in none of the carbonates analyzed were such low values found. If formed by precipitation from infiltrated lateral run-off, its signature would rather reflect a mixture of various sources, including ‘atmospheric- $\text{CO}_2$ ’, ‘marine- $\text{CO}_2$ ’ and ‘SOM- $\text{CO}_2$ ’, and thus might have an ‘intermediate’  $\delta^{13}\text{C}$  value, which is commensurate with the values that were found.

### 5.3. Radiocarbon dating

Organic matter fractions were calibrated using OxCal against IntCal20 (see Table 3 and Fig. 12). Given the inferred origin of this organic matter in the units 6, 7, 13 and 15 (see 5.1), the calibration process assumes that it came from an aquatic environment (shallow lagoon and/or brine-filled pit) in which gas exchange had resulted in an isotopic composition of dissolved  $\text{CO}_2$  that was similar to that of the atmosphere. The alternative, a significant ‘marine reservoir effect’, is highly improbable. In such scenario, the resultant ages are completely incompatible with the *terminus ante quem* set by the Roman villa (see introduction). Moreover, the non-reservoir corrected ages fit remarkably well into the time frame set by both the charcoal dating and the *terminus ante quem*.

For shells a marine reservoir effect ( $R$ , in yr) must be taken into account and secondary carbonates may also have a more or less prominent ‘marine’ origin, for which reason these carbonates have been calibrated

against both curves (see Fig. 12 and Table 3). A first complication is that the reservoir effect varies depending on the local conditions (Siani et al., 2000). Reimer & McCormac (2002) assume a global  $R$  value in the order of 400 years, with the addition of a small  $\Delta R$  value for the local Mediterranean environment (see Section 3.5). Meanwhile, Lowe et al. (2007) concluded that ‘radiocarbon dating of marine records is particularly problematic because of the pervasive and, at present, poorly constrained marine reservoir effects.’ For example, Sabatier et al. (2010) found a large  $R$  value of about 940 yr for shells from a lagoon near Montpellier in southern France. In more open lagoonal environments the  $R$  value was lower at slightly over 600 yr, and similar to values found by Siani et al. (2000). Comparison of the radiocarbon ages that we obtained for shells and organic fractions from units 6 and 13, respectively, indicates that the offset is rather similar (c. 650 years) and considerably exceeds the  $R$  based on the Correction Database ( $\Delta R = 127 \pm 28$  years).

In most units, secondary carbonates have a mixed origin (types 3 and 4), which is a second complication preventing a reliable calibration. This is demonstrated by the results for the various carbonates from unit 13: if they were all of ‘marine’ origin, their ages would be similar. The only exception is formed by unit 6 in which their ages are very similar to those for shells, confirming their ‘marine’ origin (type 3) and thus allowing for calibration of their age against the Marine20 curve. This similarity allows for another conclusion which is that the C isotopic composition of the secondary carbonates was seemingly not affected by atmospheric  $\text{CO}_2$  that through gas exchange entered the brine, contrary to that of the labile organic matter.

In summary, the most reliable calibrated ages are those for samples that are dominantly composed of labile organic matter (6, 7, 13, and 15) or charcoal samples (16), while the uncertainty about the marine reservoir effect and the mixed origin of most secondary carbonates seriously limit the use of carbonates for radiocarbon dating.

### 5.4. Briquetage, a precursor of salterns or an artisanal, coeval type of salt production?

Based on the dates obtained, the period over which the briquetage system was operative at Puntone can be defined. Its start predates the stratigraphic unit 16 that contains the charcoal dated to 1107–841 cal BCE, thus falling between the Late Bronze Age and the Early Iron Age, almost contemporary with the birth of the nearby city of Populonia (Quondam, 2020; Milletti, 2015). This evidence finds a strict parallel in the more southern Early Iron Age ‘briquetage sites’ recorded along the coast (Fig. 13), which are thought to have been under the control of the Early States of Tarquinia and Cerveteri (Alessandri et al., 2019; Pacciarelli, 2010; Belardelli, 2013).

The briquetage system at Puntone came to an end at the closure of phase 4 which, based on the results for the organic matter from this phase, dates to 343–59 cal BCE. Results for the secondary carbonates and shells in unit 6 suggest a somewhat earlier age, but the size of the marine reservoir effect may very well be greater than generally assumed (see discussion in Section 5.3). Anyway, the radiocarbon dates indicate that the briquetage continued for a considerable time and at least until the second half of the 4th century BCE but perhaps even till shortly before the 1st century BCE, when a rural Roman villa was constructed on top of its remains (Balestri & Magagnoli, 1981; Paribeni, 1985). In summary, the results show that the technique was in use during the heydays of the Iron Age Early States in this region and may well have continued into the Late Roman Republican Age.

Environmental reconstructions of the landscape around Populonia show the presence of two lagoons near the city (Isola 2009). According to some authors, these may have been partially used as salterns in Roman times. However, the first direct evidence for ancient salterns dates to Medieval Times (Carusi, 2008). Further south, an abandoned saltern is still visible along the coast near Tarquinia. Here, the first direct evidence for the age of the salterns points to a Medieval origin, although some topographical considerations suggest that it could have already

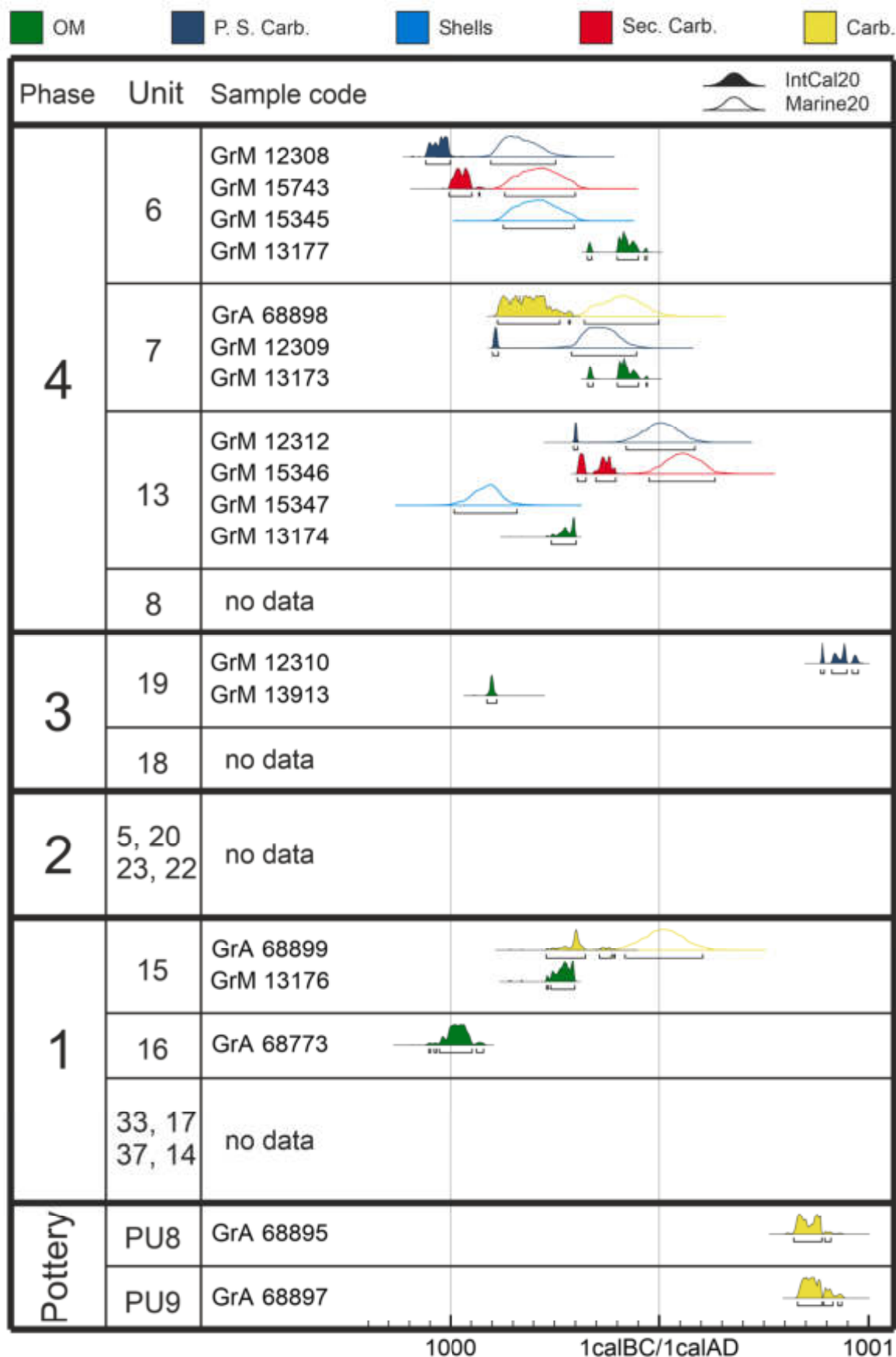


Fig. 12. Calibrated radiocarbon ages of the various samples. OM = Organic matter (LOM: 6, 7, 13, and 15; ROM: 19; Charcoal: 16); P.S. Carb. = Poorly soluble carbonate fraction; Sec. Carb. = Hand-picked secondary carbonate aggregates; Carb. = Total carbonates fine earth fractions. Calibrations are against the IntCal curve and the Marine20 curve ( $\Delta R = -127 \pm 28$  yr).





Fig. 13. Salt map. Relevant sites cited in the text. Early State territory boundaries after Amoroso, 2016; Di Paola and Piani, 2012; ancient lake/lagoon reconstructions after Isola, 2009; Alessandri, 2013; Van Gorp, Sevink, and Van Leusen, 2020.

been in use at the time when the Etruscan city of Tarquinia flourished (Bonghi Jovino, 2002). Other salterns were known to have existed both north and south of the Tiber mouth, under the control of the cities of Veii and Rome, respectively (Giovannini, 1985). The date of the beginning of their use is uncertain but they are already cited by Latin sources in the framework of the early wars between Veio and Rome. When Romolo defeated Veio, the latter lost the salterns as a consequence (Plut. *Rom.* 25, 6; Dion. Hal. *Ant. Rom.* 2, 55, 5). Hence, it is not surprising that palynological data collected in the lagoons in the Tiber mouth area show an increased salinity already in the 7<sup>th</sup> century BCE, possibly caused by their artificial opening to let in seawater (Di Rita et al., 2010; Bellotti

et al., 2011). It is certain that these salterns were in use during the Roman Republican and Imperial Ages (Pannuzi, 2013; Grossi et al., 2015).

## 6. Conclusions

This paper concerns an attempt to date the early production of salt at Puntone in Central Tuscany, which was based on leaching of saline lagoonal sediment over a sieve placed over a pit in which the brine was collected, followed by boiling the brine in ceramic vessels to produce massive salt, the so-called briquetage technique. Given the absence of



stratigraphies containing readily datable artefacts or organic materials, we decided to study the sedimentary sequence encountered in and around an infilled former brine pit. The first topic of this paper concerned the origin of the carbonates and organic matter encountered in this phased sedimentary sequence and their potential for radiocarbon dating the phases that we could distinguish. We employed a range of methods, that together provided quite detailed insights into their composition and origin, but also showed that their radiocarbon dating is often problematic.

The origin of the carbonates turned out to be complex. In most instances a reliable quantification of individual components was impossible, nor was it possible to separate and radiocarbon date these components (shell fragments, detrital carbonates, and several types of secondary carbonates, see Section 5.2). An exception is formed by the shells found in the stratigraphically younger units but in most stratigraphic units shells are truly scarce or absent. The bulk of the secondary carbonates was found to consist of a mixture of carbonates that precipitated from brine in the pit in a more or less anoxic environment (coeval carbonates), and of younger, post-briquetage carbonates that precipitated at some depth in the archaeological strata. The observed inverse relationship between the age of the secondary carbonates and their stratigraphic position is remarkable and demonstrates the importance of this recent precipitation of carbonate in the deeper strata.

It is only in the youngest pit fill units, in which the post-briquetage accumulation of secondary carbonates is minimal or even absent, that 'coeval secondary carbonates' truly dominate. Unfortunately, uncertainty about the magnitude of the 'marine reservoir effect' hampers a reliable calibration of the ages obtained for these materials and for the shells. This effect seems to be of a similar order of magnitude as observed elsewhere in comparable Mediterranean lagoonal environments: c. 650 years.

The microbial DNA analyses and C isotopic data together show that most of the organic matter fractions are largely composed of labile organic matter that was fossilized upon its burial by more recent materials, thus providing a reliable indication for the age of the units holding this material. The IntCal20 calibrated ages should be seen as a *terminus ante quem* rather than a precise age of the respective stratigraphic units, since the fractions may also contain some older, more stable organic matter. Nevertheless, the match between the sequence of calibrated ages and the time frame derived from the archaeological materials and radiocarbon dates of the charcoal encountered in early strata, is remarkable. It shows that the briquetage continued well into the Early Republican period of Rome.

The second topic concerns the age of the briquetage system and its relations with saltern-based production systems. The briquetage site at Puntone is only one of the many briquetage sites in the territories of Iron Age Early States like Populonia, Cerveteri, and Tarquinia, but counts among the very rare sites for which the latest phase of production could be dated. At Puntone this briquetage continued well into the Early Republican period, suggesting that briquetage formed a continuous basis for the salt supply of these Early States. On the contrary, Veio and Rome probably produced their salt using the saltern technique. For the moment, the overall evidence thus suggests that both techniques were simultaneously in use from the very beginning of the Early States till well into the Early Republican period. That different approaches were used in salt production might have been due to the differences in the environmental niches required for the briquetage and salterns, and the availability of the necessary know-how.

Evidently, these hypotheses need further confirmation by studies of other briquetage sites in Central Italy. Unfortunately, the dating of their later phases is likely to be impeded by the same limitations that were encountered at Puntone: the absence of typologically well-datable artefacts and of charcoal or other materials that can be readily radiocarbon dated. Our research shows that these limitations can be overcome by radiocarbon dating materials that are selected on the basis of a thorough study of the various briquetage materials and that labile organic matter

(LOM) may well be the key material for such dating.

## Funding

Microscopical, physical, chemical, and microbial analyses were funded by the Institute for Biodiversity and Ecosystem Dynamics (IBED), University of Amsterdam (Netherlands); X-ray diffraction, Sr isotope, and SEM/EDS analyses were funded by the Osservatorio Vesuviano, Istituto Nazionale di Geofisica e Vulcanologia (INGV), Naples (Italy); and C isotope analyses were funded by the Centre for Isotope Research (CIO), University of Groningen (Netherlands).

## Declaration of Competing Interest

The authors declare that they have no known competing financial interests or personal relationships that could have appeared to influence the work reported in this paper.

## Acknowledgements

The investigations were carried out in the context of the PhD research of Maria Rosaria Cinquegrana at GIA (Convenzione prot. SAR-TOS n. 3794 del 14/3/2016; Concessione DG-ABAP: prot. 3854 del 9/2/2017). Special thanks are due to Dott.ssa Bianca Maria Aranguren Torini of the responsible Soprintendenza for her support. Lastly, we acknowledge the two anonymous reviewers for suggestions and comments, which allowed us to improve this paper.

## Appendix A. Supplementary data

Supplementary data to this article can be found online at <https://doi.org/10.1016/j.jasrep.2021.103055>.

## References

- Alessandri, L., 2013. Latium Vetus in the Bronze Age and Early Iron Age / Il Latium Vetus nell'età del Bronzo e nella prima età del Ferro. BAR Int. Ser. 2565, Oxford.
- Alessandri, L., Achino, K.F., Attema, P.A.J., de Novaes Nascimento, M., Gatta, M., Rolfo, M.F., Sevinck, J., Sottili, G., van Gorp, W., Biehl, P.F., 2019. Salt or Fish (or Salted Fish)? The bronze age specialised sites along the tyrrhenian coast of central Italy: New insights from Caprolace settlement. PLoS ONE 14 (11), e0224435.
- Amoroso, A., 2016. Settlement patterns in South Etruria and Latium Vetus. In: Attema, P.A.J., Seubers, J.F., Willemsen, S.L. (Eds.), Early states, territories and settlements in protohistoric Central Italy: Proceedings of a specialist conference at the Groningen Institute of Archaeology of the University of Groningen, 2013. Corollaria Crustumina Vol. 2, Barkhuis, Groningen, The Netherlands, 83–100.
- Aranguren, B.M., 2002. Il golfo di Follonica in età protostorica: l'idrografia antica e i sistemi insediamentali. Atti del V Incontro di Studi di Preistoria e Protostoria in Etruria 111–122.
- Aranguren, B.M., Castelli, S., 2011. Fra mare e laguna: ipotesi interpretative per il sito produttivo di Portigliotti, Scarlino (GR). Atti del 4o Convegno Nazionale di Etnoarcheologia, Roma 2006. BAR Int. Ser. 2235, 9–16.
- Aranguren, B.M., Cinquegrana, M.R., De Bonis, A., Guarino, V., Morra, V., Pacciarelli, M., 2014. Le strutture e lo scarico di olle del Puntone Nuovo di Scarlino (GR), e i siti costieri specializzati della protostoria mediotirrenica. Riv. Sci. Preist. LXIV 227–259.
- Arienzo, I., Carandente, A., Di Renzo, V., Belviso, P., Civetta, L., D'Antonio, M., Orsi, G., 2013. Sr and Nd isotope analysis at the Radiogenic Isotope Laboratory of the Istituto Nazionale di Geofisica e Vulcanologia Sezione di Napoli—Osservatorio Vesuviano. Rapporti Tecnici INGV 260:1–18. <https://istituto.ingv.it/lingv/produzione-scientifica/rapporti-tecnici-ingv/archivio/rapporti-tecnici>.
- Attema, P.A.J., Alessandri, L., 2012. Salt production on the Tyrrhenian coast in South Lazio (Italy) during the Late Bronze Age: Its significance for understanding contemporary society. In: Nikolov, V., Barvarov, K. (Eds.), Salt and Gold: The Role of Salt in Prehistoric Europe. Provadia-Veliko Tarnovo, pp. 287–300.
- Balestri, A., Magagnoli, R., 1981. La storia del Golfo di Follonica, I. Follonica.
- Baratti, G., 2010. Un sito per la produzione del sale sulla spiaggia di Baratti (area Centro Velico) 950 alla fine dell'età del Bronzo. Mater. Populonia 9, 243–260.
- Barbaranelli, F., 1956. Villaggi villanoviani dell'Etruria meridionale marittima. Boll. Paletnol. Ital. 65, 455–489.
- Beam, J.P., Becraft, E.D., Brown, J.M., Schulz, F.P., Jarett, J.K., Beznidt, O., Poulton, N.J., Clark, K., Dunfield, P.F., Ravin, N.V., Spear, J.R., Hedlund, B.P., Korman, K.A., Sievert, S.A., Elshahed, M.S., Barton, H.A., Stott, M.B., Eisen, J.A., Moser, D.P., Onstott, T.C., Woyke, T., Stepanauskas, R., 2020. Ancestral absence of electron



- transport chains in Patescibacteria and DPANN. *bioRxiv*. doi.org/10.1101/2020.04.07.029462.
- Belardelli, C., 2013. Coastal and underwater late urnfield sites in South Etruria. *Skyllis* 1, 5–17.
- Bellotti, P., Calderoni, G., Di Rita, F., D'Orefice, M., D'Amico, C., Esu, D., Magri, D., Martinez, M.P., Tortora, P., Valeri, P., 2011. The Tiber river delta plain (Central Italy): coastal evolution and implications for the ancient Ostia water settlement. *Holocene* 21 (7), 1105–1116. <https://doi.org/10.1177/0959683611400464>.
- Bintliff, J., 2016. Early states in the Mediterranean Iron Age (ca. 1000–400 BC). In: Attema, P.A.J., Seubers, J.F., Willemsen, S.L. (Eds.), *Early states, territories and settlements in protohistoric Central Italy: Proceedings of a specialist conference at the Groningen Institute of Archaeology of the University of Groningen*, 2013. *Corollaria Crustumina* Vol. 2, Barkhuis, Groningen, The Netherlands, 1–8.
- Bonghi Jovino, M., 2002. Tarquinia, Sale e Saline. *Quaderni Di Acme* 55, 27–37.
- Boschetti, T., Venturini, G., Toscani, L., Barbieri, M., Mucchino, C., 2005. The Bagni di Lucca thermal waters (Tuscany Italy): an example of Ca-SO<sub>4</sub> waters with high Na/Cl and low Ca/SO<sub>4</sub> ratios. *J. Hydrol.* 307 (1–4), 270–293. <https://doi.org/10.1016/j.jhydrol.2004.10.015>.
- Boutton, T.W., Archer, S.R., Midwood, A.J., Zitzer, S.F., Bol, R., 1998.  $\delta^{13}C$  values of soil organic carbon and their use in documenting vegetation change in a subtropical savanna ecosystem. *Geoderma* 82 (1–3), 5–41. [https://doi.org/10.1016/S0016-7061\(97\)00095-5](https://doi.org/10.1016/S0016-7061(97)00095-5).
- Bronk Ramsey, C., 2020. Oxcal 4.4. <https://c14.arch.ox.ac.uk/oxcal/OxCal.html>.
- Cappuccini, L., 2011. Il litorale tirrenico a sud di Populonia in epoca etrusca. In: Paoletti, O. (Ed.), *La Corsica e Populonia. Atti del 28 Convegno di Studi Etruschi ed Italici: Bastia, Aléria, Piombino, Populonia, 25–29 ottobre 2011*, 567–590.
- Carusi, C., 2008. Intorno alla produzione di sale a Populonia e Nell'Ager Cosanus: due casi di studio a confronto. *Mater. Populonia* 7, 7–16.
- Chong, J., Liu, P., Zhou, G., Xia, J., 2020. Using MicrobiomeAnalyst for comprehensive statistical, functional, and meta-analysis of microbiome data. *Nat. Protoc.* 15 (3), 799–821. <https://doi.org/10.1038/s41596-019-0264-1>.
- Cinquegrana, M.R. PhD thesis University of Groningen, in prep.
- Cornamusi, G., 2002. Compositional evolution of the Macigno Fm. of southern Tuscany along a transect from the Tuscan coast to the Chianti Hills. *Boll. Soc. Geol. Ital. Spec.* 1, 365–374.
- Darnaude, A.M., Salen-Picard, C., Polunin, N.V., Harmelin-Vivien, M.L., 2004. Trophodynamic linkage between river runoff and coastal fishery yield elucidated by stable isotope data in the Gulf of Lions (NW Mediterranean). *Oecologia* 138 (3), 325–332. <https://doi.org/10.1007/s00442-003-1457-3>.
- Dee, M.W., Palstra, S.W.L., Aerts-Bijma, A.T., Bleeker, M.O., De Bruijn, S., Ghebru, F., Jansen, H.G., Kuitens, M., Paul, D., Richiè, R.R., Spiersma, J.J., Scifo, A., Van Zonneveld, D., Verstappen-Dumoulin, B.M.A.A., Wietzes-Land, P., Meijer, H.A.J., 2020. Radiocarbon dating at Groningen: New and updated chemical pretreatment procedures. *Radiocarbon* 62 (1), 63–74. <https://doi.org/10.1017/RDC.2019.101>.
- Deneke, E., Günther, K., 1981. Petrography and arrangement of Tertiary graywacke and sandstone sequences of the Northern Apennines. *Sediment. Geol.* 28 (3), 189–230. [https://doi.org/10.1016/0037-0738\(81\)90065-8](https://doi.org/10.1016/0037-0738(81)90065-8).
- Dinelli, E., Lucchini, F., Mordenti, A., Paganelli, L., 1999. Geochemistry of Oligocene-Miocene sandstones of the northern Apennines (Italy) and evolution of chemical features in relation to provenance changes. *Sediment. Geol.* 127 (3–4), 193–207. [https://doi.org/10.1016/S0037-0738\(99\)00049-4](https://doi.org/10.1016/S0037-0738(99)00049-4).
- Di Paola, G., Piani, P., 2012. Confini e fortezze d'altura del territorio di Populonia: indagini preliminari. *Aristonothos. Scritti per il Mediterraneo antico* 5, 261–297.
- Di Rita, F., Celant, A., Magri, D., 2010. Holocene Environmental Instability in the Wetland North of the Tiber Delta (Rome, Italy): Sea-Lake-Man Interactions. *J. Paleolimnol.* 44 (1), 51–67. <https://doi.org/10.1007/s10933-009-9385-9>.
- Douka, K., Higham, T.F., Hedges, R.E., 2010. Radiocarbon dating of shell carbonates: old problems and new solutions. *Munibe Suplemento* 31, 18–27.
- Dridi, B., Fardeau, M.L., Olivier, B., Raoult, D., Drancourt, M., 2012. *Methanomassiliococcus luminyensis* gen. nov., sp. nov., a methanogenic archaeon isolated from human faces. *Int. J. Syst. Evol. Microbiol.* 62, 1902–1907. <https://doi.org/10.1099/ijs.0.033712-0>.
- Duchaufour, R., 2012. *Pedology: pedogenesis and classification*. Springer Science & Business Media.
- Ettwig, K.F., Butler, M.K., De Paslier, D., Pelletier, E., Manguot, S., Kuypers, M.M.M., Schreiber, F., Dutilh, B.E., Zedelius, J., de Beer, D., Gloerich, J., Wessels, H.J.C.T., van Alen, T., Luesken, F., Wu, M.L., van de Pas-Schoonen, K.T., Op den Camp, H.J.M., Janssen-Megens, E.M., Francoijs, K.-J., Stunnenberg, H., Weissenbach, J., Jetten, M.S.M., Strous, M., 2010. Nitrite-driven anaerobic methane oxidation by oxygenic bacteria. *Nature* 464 (7288), 543–548. <https://doi.org/10.1038/nature08883>.
- Evangelopoulos, A., Spyarakos, E., Koutsoubas, D., 2009. Phytoplankton and macrofauna in the low salinity ponds of a productive solar saltworks: spatial variability of community structure and its major abiotic determinants. *Global NEST J.* 11 (1), 64–72.
- Gandolfi, G., Paganelli, L., 1975. Il litorale toscano fra Livorno e il Promontorio di Piombino (Area Campione Alto Tirreno). *Composizione, provenienza e dispersione delle sabbie*. *Boll. Soc. Geol. Ital.* 94, 1833–1854.
- Giovannini, A., 1985. "Le Sel et La Fortune de Rome." *Athenaeum* 63, 373–386.
- Giroldini, P., 2012. Between land and sea: a GIS based settlement analysis of the ancient coastal lagoon of Piombino (Tuscany, Italy). *eTopoi Spec.* 3, 383–389.
- Grossi, M.C., Sivilli, S., Arnoldus-Huyzendveld, A., Facciolo, A., Rinaldi, M.L., Ruggeri, D., Morelli, C., 2015. A Complex Relationship between Human and Natural Landscape: A Multidisciplinary Approach to the Study of the Roman Saltworks in 'Le Vignole - Interporto' (Maccarese, Fiumicino - Roma). In: Brigand, R., Weller, O. (Eds.), *Archaeology of Salt: Approaching an Invisible Past*, Sidestone press, 83–101.
- Harding, A., 2013. *Salt in prehistoric Europe*. Sidestone Press.
- Harding, A., 2014. The Prehistoric Exploitation of Salt in Europe. *Geol. Q.* 58 (3), 591–596. <https://doi.org/10.73306/gq.1164>.
- Harmelin-Vivien, M., Loizeau, V., Mellon, C., Bekker, B., Arlhaç, D., Bodiguel, X., Ferratona, F., Hermand, R., Philippon, X., Salen-Picard, C., 2008. Comparison of C and N stable isotope ratios between surface particulate organic matter and microphytoplankton in the Gulf of Lions (NW Mediterranean). *Cont. Shelf Res.* 28 (15), 1911–1919. <https://doi.org/10.1016/j.csr.2008.03.002>.
- Heaton, T.J., Köhler, P., Butzin, M., Bard, E., Reimer, R.W., Austin, W.E.N., Bronk Ramsey, C., Grootes, P.M., Hughes, K.A., Kromer, B., Reimer, P.J., Adkins, J., Burke, A., Cook, M.S., Olsen, J., Skinner, L.C., 2020. Marine20—the marine radiocarbon age calibration curve (0–55,000 cal BP). *Radiocarbon* 62 (4), 779–820. <https://doi.org/10.1017/RDC.2020.68>.
- Hocquet, J.C., Sarrazin, J.L., 2006. *Le sel de la Baie: Histoire, archéologie, ethnologie des sels atlantiques*. Presses universitaires de Rennes, Rennes, France. doi.org/10.4000/books.pur.7581.
- Isola, C., 2009. *Le Lagune Di Populonia Dall'antichità Alle Bonifiche*. In: Cambi, F., Cavari, F., Mascione, C. (Eds.), *Materiali Da Costruzione e Produzione Del Ferro*. Bari, pp. 163–169.
- Klindworth, A., Pruesse, E., Schweer, T., Peplies, J., Quast, C., Horn, M., Glöckner, F.O., 2013. Evaluation of general 16S ribosomal RNA gene PCR primers for classical and next-generation sequencing-based diversity studies. *Nucl. Acids Res.* 41: e1. doi: 10.1093/nar/gks808.
- Krauskopf, K.B., 1967. *Introduction to Geochemistry*. McGraw-Hill, New York.
- Leoni, L., Sartori, F., 1996. Mineralogy, chemistry and grain size composition of the bottom sediments in the Elba-Argentario basin (Southern Tuscany, Italy): contribution to assessment of sediment sources and dynamics. *Atti. Soc. Tosc. Sci. Nat. Mem. Ser. A* 103, 27–40.
- Leoni, L., Sartori, F., 1997. Heavy metal and arsenic distributions in sediments of the Elba-Argentario basin, southern Tuscany, Italy. *Environ. Geol.* 32 (2), 83–92.
- Lowe, J.J., Blockley, S., Trincardi, F., Ascoli, A., Cattaneo, A., Matthews, I.P., Pollard, M., Wulf, S., 2007. Age modelling of late Quaternary marine sequences in the Adriatic: towards improved precision and accuracy using volcanic event stratigraphy. *Cont. Shelf Res.* 27 (3–4), 560–582. <https://doi.org/10.1016/j.csr.2005.12.017>.
- Lowe, B., 2018. Manilius and the Logistics of Salting in the Roman World. *J. Marit. Archaeol.* 13 (3), 467–480. <https://doi.org/10.1007/s11457-018-9220-4>.
- Ludwig, W., Strunk, O., Westram, R., Richter, L., Meier, H., Yadhukumar, Buchner, A., Lai, T., Steppi, S., Jobb, G., Förster, W., Brettiske, L., Gerber, S., Ginhart, A.W., Gross, O., Grumann, S., Hermann, S., Jost, R., König, A., Liss, T., Lüssmann, R., May, M., Nonhoff, B., Reichel, B., Strehlow, R., Stamatakis, A., Stuckmann, N., Vilbig, A., Lenke, M., Ludwig, T., Bode, A., Schleifer, K.H., 2004. ARB: a software environment for sequence data. *Nucleic Acids Res.* 32, 1363–1371. DOI: 10.1093/nar/gkh293.
- Madigan, M.T., Bender, K.S., Buckley, D.H., Sattley, W.M., Stahl, D.A., 2019. *Brook Biology of Microorganisms*, 15th Edition. Pearson Education Limited, Harlow, United Kingdom.
- McBride, M.B., 1994. *Environmental Chemistry of Soils*. Oxford Univ. Press, New York/Oxford.
- McBride, E.F., Parea, G.C., 2001. Origin of highly elongate, calcite-cemented concretions in some Italian coastal beach and dune sands. *J. Sediment. Res.* 71 (1), 82–87. <https://doi.org/10.1306/041900710082>.
- Millèri, M., 2015. La Nascita Di Populonia: Dati e Ipotesi Sullo Sviluppo Della Città Etrusca All'alba Del Primo Millennio a.C. In: Rendeli, M. (Ed.), *Le Città Visibili. Atti Del Seminario Internazionale in Onore Di Gilda Bartoloni e Alberto Moravetti*, Officina edizioni, 59–96.
- Mook, W.G., Van Der Plicht, J., 1999. Reporting  $^{14}C$  activities and concentrations. *Radiocarbon* 41 (3), 227–239. <https://doi.org/10.1017/S0033822200057106>.
- Nisi, B., Bucciatti, A., Vaselli, O., Perini, G., Tassi, F., Minissale, A., Montegrossi, G., 2008. Hydrogeochemistry and strontium isotopes in the Arno River Basin (Tuscany, Italy): constraints on natural controls by statistical modeling. *J. Hydrol.* 360 (1–4), 166–183. <https://doi.org/10.1016/j.jhydrol.2008.07.030>.
- Osman, J.R., Regeard, C., Badel, C., Fernandes, G., DuBow, M.S., 2019. Variation of bacterial biodiversity from saline soils and estuary sediments present near the Mediterranean Sea coast of Camargue (France). *Antonie Van Leeuwenhoek* 112 (3), 351–365. <https://doi.org/10.1007/s10482-018-1164-z>.
- Pacciarelli, M., 2010. Verso i Centri Proturani. Situazioni a Confronto Da Etruria Meridionale, Campania e Calabria. In: Cardarelli, A., Cazzella, A., Frangipane, M., Peroni, R., *Le Ragioni Del Cambiamento/Reasons for Change*, Atti Del Convegno Internazionale 15, Scienze dell'Antichità, Roma, 371–416.
- Pannuzi, S., 2013. La Laguna Di Ostia : Produzione Del Sale e Trasformazione Del Paesaggio Dall'età Antica All'età Moderna. *Mélanges de l'école Française de Rome. Moyen Âge* 125 (2). doi.org/10.4000/mefm.1507.
- Paribeni, E., 1985. *Scarlino. Studi e Materiali* V, 372.
- Pennisi, M., Bianchini, G., Muti, A., Kloppmann, W., Gonfiantini, R., 2006. Behaviour of boron and strontium isotopes in groundwater-aquifer interactions in the Cornia Plain (Tuscany, Italy). *Appl. Geochem.* 21 (7), 1169–1183. <https://doi.org/10.1016/j.apgeochem.2006.03.001>.
- Pigati, J.S., 2013. Radiocarbon Dating of Terrestrial Carbonates. W.J. Rink, J. Thompson (Eds.), *Encyclopedia of Scientific Dating Methods*, Springer, Netherlands, 1–9.
- Pranzini, E., 1978. Studi di geomorfologia costiera: VI. La dispersione delle sabbie carbonatiche di discarica a sud di Rosignano Solvay. *Boll. Soc. Geol. Ital.* 97, 439–450.
- Pruesse, E., Peplies, J., Glöckner, F.O., 2012. SINA: accurate high-throughput multiple sequence alignment of ribosomal RNA genes. *Bioinformatics* 28, 1823–1829. <https://doi.org/10.1093/bioinformatics/bts252>.



- Pusceddu, A., Sarà, G., Armeni, M., Fabiano, M., Mazzola, A., 1999. Seasonal and spatial changes in the sediment organic matter of a semi-enclosed marine system (W-Mediterranean Sea). *Hydrobiologia* 397, 59–70.
- Quero, G.M., Perini, L., Pesole, G., Manzari, C., Lionetti, C., Bastianini, M., Marini, M., Luna, G.M., 2017. Seasonal rather than spatial variability drives planktonic and benthic bacterial diversity in a microtidal lagoon and the adjacent open sea. *Mol. Ecol.* 26 (21), 5961–5973. <https://doi.org/10.1111/mec.2017.26.issue-2110.1111/mec.14363>.
- Quondam, F., 2020. L'Italia Dei Centri Proto-Urbani: Percorsi Regionali a Confronto. *Gaia* 22–23.
- Railsback, L.B., 1999. Patterns in the compositions, properties, and geochemistry of carbonate minerals. *Carbonate. Evaporite*. 14 (1), 1–20. <https://doi.org/10.1007/BF03176144>.
- Raiswell, R., Canfield, D.E., Berner, R.A., 1994. A comparison of iron extraction methods for the determination of degree of pyritisation and the recognition of iron-limited pyrite formation. *Chem. Geol.* 111 (1–4), 101–110. [https://doi.org/10.1016/0009-2541\(94\)90084-1](https://doi.org/10.1016/0009-2541(94)90084-1).
- Reimer, P.J., McCormac, F.G., 2002. Marine radiocarbon reservoir corrections for the Mediterranean and Aegean Seas. *Radiocarbon* 44 (1), 159–166. <https://doi.org/10.1017/S0033822200064766>.
- Reimer, P., Austin, W.E.N., Bard, E., Bayliss, A., Blackwell, P.G., Bronk Ramsey, C., Butzin, M., Cheng, H., Edwards, R.L., Friedrich, M., Grootes, P.M., Guilderson, T.P., Hajdas, I., Heaton, T.J., Hogg, A.G., Hughen, K.A., Kromer, B., Manning, S.W., Muscheler, R., Palmer, J.G., Pearson, C., Van der Plicht, J., Reimer, R.W., Richards, D.A., Scott, E.M., Southon, J.R., Turney, C.S.M., Wacker, L., Adolphi, F., Büntgen, U., Capano, M., Fahrni, S., Fogtmann-Schulz, A., Friedrich, R., Köhler, P., Kudsk, S., Miyake, F., Olsen, J., Reinig, F., Sakamoto, M., Sookdeo, A., Talamo, S., 2020. The IntCal20 Northern Hemisphere radiocarbon age calibration curve (0–55 cal kBP). *Radiocarbon* 62, 725–757. <https://doi.org/10.1017/RDC.2020.41>.
- Renzi, M., Bigongiari, N., Focardi, S.E., 2015. Baseline levels of trace elements in coastal sediments from the central Mediterranean (Tuscany, Italy). *Chem. Ecol.* 31 (1), 34–46. <https://doi.org/10.1080/02757540.2014.943200>.
- Renzi, M., Provenza, F., Pignattelli, S., Cilenti, L., Specchiulli, A., Pepi, M., 2019. Mediterranean coastal lagoons: the importance of monitoring in sediments the biochemical composition of organic matter. *Int. J. Environ. Res. Pub. He.* 16 (18), 3466. <https://doi.org/10.3390/ijerph16183466>.
- Sabatier, P., Dezileau, L., Blanchemanche, P., Siani, G., Condomines, M., Bentaleb, I., Piquès, G., 2010. Holocene variations of radiocarbon reservoir ages in a Mediterranean lagoonal system. *Radiocarbon* 52 (1), 91–102. <https://doi.org/10.1017/S0033822200045057>.
- Sarti, G., Sammartino, I., Amorosi, A., 2020. Geochemical anomalies of potentially hazardous elements reflect catchment geology: An example from the Tyrrhenian coast of Italy. *Sci. Total Environ.* 714, 136870. <https://doi.org/10.1016/j.scitotenv.2020.136870>.
- Schwertmann, U., 1993. Relations between iron oxides, soil color, and soil formation. In: Bigham, J.M., Ciolkosz, E.J. (Eds): *Soil Color, Madison, WI: Soil Sci. Soc. Am., Special Publ. Nr. 31*, 51–69.
- Sevink, J., De Neef, W., Alessandri, L., Van Hall, R.L., Ullrich, B., Attema, P.A., 2021. Protohistoric briquetage at Puntone (Tuscany, Italy): principles and processes of an industry based on the leaching of saline lagoonal sediments. *Geochronology* 36 (1), 54–71. <https://doi.org/10.1002/gea.v36.110.1002/gea.21820>.
- Siani, G., Paterne, M., Arnold, M., Bard, E., Métié, B., Tisnerat, N., Bassinot, F., 2000. Radiocarbon Reservoir Ages in the Mediterranean Sea and Black Sea. *Radiocarbon* 42 (2), 271–280. <https://doi.org/10.1017/S0033822200059075>.
- Tencariu, F.A., Alexianu, M., Cotiugă, V., Vasilache, V., Sandu, I., 2015. Briquetage and salt cakes: an experimental approach of a prehistoric technique. *J. Archaeol. Sci.* 59, 118–131. <https://doi.org/10.1016/j.jas.2015.04.016>.
- Thijs, S., Op de Beeck, M., Beckers, B., Truyens, S., Stevens, V., Van Hamme, J.D., Weyens, N., Vangronsveld, J., 2017. Comparative evaluation of four bacteria-specific primer pairs for 16S rRNA gene surveys. *Front. Microbiol.* 8, 494. <https://doi.org/10.3389/fmicb.2017.00494>.
- Tian, R., Ning, D., He, Z., 2020. Small and mighty: adaptation of superphylum Patescibacteria to groundwater. *Microbiome*, 8 (1). Turner, J.V., (1982) Kinetic fractionation of carbon-13 during calcium carbonate precipitation. *Geochim. Cosmochim. Acta* 46, 1183–1191. <https://doi.org/10.1186/s40168-020-00825-w>.
- Tisnerat-Laborde, N., Montagna, P., McCulloch, M., Siani, G., Silenzi, S., Frank, N., 2013. A high-resolution coral-based  $\Delta 14C$  record of surface water processes in the western Mediterranean Sea. *Radiocarbon* 55 (2–3), 1617–1630. [https://doi.org/10.2458/azu\\_js\\_rc.55.16397](https://doi.org/10.2458/azu_js_rc.55.16397).
- Usiglio, M., 1849. Études sur la composition de l'eau de la Méditerranée et sur l'exploitation des sels qu'elle contient. *Ann. Chim. Phys.* 27, 172–191.
- Van der Plicht, J., Hogg, A., 2006. A note on reporting radiocarbon. *Quat. Geochronol.* 1 (4), 237–240. <https://doi.org/10.1016/j.quageo.2006.07.001>.
- Van der Plicht, J., Nijboer A.J., 2018. Around 1000 BC. Absolute dates for the Final Bronze Age – Early Iron Age transition in Italy: wiggle-match  $14C$  dating of two tree-trunk coffins from Celano. *Palaeohistoria*, 59/60 (2017/2018): 99–108. [doi.org/10.21827/5beaafbcc2bf2](https://doi.org/10.21827/5beaafbcc2bf2).
- Van Gorp, W., Sevink, J., Van Leusen, P.M., 2020. Post-Depositional Subsidence of the Avellino Tephra Marker Bed in the Pontine Plain (Lazio, Italy): implications for Early Bronze Age Palaeogeographical, Water Level and Relative Sea Level Reconstruction. *Catena* 194, 104770. <https://doi.org/10.1016/j.catena.2020.104770>.
- Vizzini, S., Mazzola, A., 2003. Seasonal variations in the stable carbon and nitrogen isotope ratios ( $13C/12C$  and  $15N/14N$ ) of primary producers and consumers in a western Mediterranean coastal lagoon. *Mar. Biol.* 142 (5), 1009–1018. <https://doi.org/10.1007/s00227-003-1027-6>.
- Xu, F., You, X., Li, Q., Liu, Y., 2019. Can Primary Ferroan Dolomite and Ankerite Be Precipitated? Its Implications for Formation of Submarine Methane-Derived Authigenic Carbonate (MDAC) Chimney. *Minerals* 9 (7), 413. <https://doi.org/10.3390/min9070413>.
- Youssef, N.H., Farag, L.F., Rinke, C., Hallam, S.J., Woyke, T., Elshahed, M.S., 2015. In silico analysis of the metabolic potential and niche specialization of candidate Phylum “Latescibacteria” (WS3). *PLoS ONE* 10 (6), e0127499. <https://doi.org/10.1371/journal.pone.0127499>.